THE ASTROPHYSICAL JOURNAL, 480:647–673, 1997 May 10

THE PHYSICS OF DUST COAGULATION AND THE STRUCTURE OF DUST AGGREGATES IN SPACE

C. DOMINIK
Leiden Observatory, P.O. Box 9513, NL-2300 RA Leiden, The Netherlands
AND
A. G. G. M. TIELENS
NASA Ames Research Center, Mail Stop 245-3, Moffett Field, CA 94035
Received 1996 September 6; accepted 1996 December 9

ABSTRACT

Even though dust coagulation is a very important dust-processing mechanism in interstellar space and protoplanetary disks, there are still important parts of the physics involved that are poorly understood. This imposes a serious problem for model calculations of any kind. In this paper, we attempt to improve the situation by including the effects of tangential forces on the contact in some detail. These have been studied in recent papers. We summarize the main results from these papers and apply them to detailed simulations of the coagulation process and of collisions between dust aggregates. Our results show the following: (1) the growth of aggregates by monomers will normally not involve major restructuring of the aggregates, (2) the classical *hit-and-stick* assumption is reasonably valid for this case, (3) collisions of aggregates with each other or with large grains can lead to significant compaction, and (4) the results can be easily understood in terms of critical energies for different restructuring processes. We also derive a short summary that may be used as a recipe for determining the outcome of collisions in coagulation calculations. It is shown that turbulent velocity fields in interstellar clouds are capable of producing considerably compressed aggregates, while the small aggregates forming early on in the solar nebula will not be compacted by collisions. However, compaction provides an important energy sink in collisions of larger aggregates in the solar nebula.

Subject headings: circumstellar matter — dust, extinction — interplanetary medium — ISM: clouds — solar system: formation

1. INTRODUCTION

Coagulation of submicron-sized dust grains is of importance in a variety of physical environments. In sooting flames or fires, coagulation dominates the grain growth and hence the radiative budget and flame temperature and thereby controls, for example, motor efficiency as well as atmospheric pollution (see, e.g., Hucknal 1985; Smyth & Miller 1987). In industrial milling, it determines the outcome of grinding processes (see, e.g., Beke 1981; Austin, Kimpel, & Lockie 1984). Adhesion plays an important role in the growth of aerosols and thus in the atmospheric energy budget (Marlow 1980). Powders have many industrial applications, including catalysis, pharmaceutical, cosmetic, and foodstuff. Adhesive influences govern many aspects of these powders such as mixing and flow (Rhodes 1984). Grain-grain interactions also control the static stress distribution of granular media, including rocks, clays, and rubble, as well as sugar and wheat, and hence their packing and transport (Nedderman 1992; Veale 1972; Kendall 1993).

In astrophysics, coagulation plays an important role in the grain size distribution in a variety of environments. For example, interstellar grains are known to be larger inside dense clouds, and this is generally attributed to the increased coagulation rate in such dense regions (see Tielens 1989). The importance of coagulation in the ISM is also emphasized by the ease with which large ($\simeq$1000 Å) grains are shattered into small ($\simeq$100 Å) fragments by interstellar shocks (Jones, Tielens, & Hollenbach 1996). Various theoretical interstellar dust models have been developed in recent years based upon the predominance of porous or fluffy particles (see Mathis & Whiffen 1989). Coagulation has also played an important role in the assemblage of the solar system. Submicron-sized, newly condensed grains as well as surviving interstellar grains have been put together in a gentle fashion in the protosolar nebula through weak adhesive forces into millimeter- or centimeter-sized bodies before raining out into a thin dust disk (Weidenschilling & Cuzzi 1993). Initially, in this dust disk, coagulation continued to dominate particle growth all the way to the formation of kilometer-sized planetesimals, when gravity took over. A record of the importance of coagulation in planet formation has survived in the predominance of dust rims on meteoritic chondrules and the microstructure of interplanetary dust particles, both of which betray their collisional origins (Brownlee 1979). The loose agglomerated structure of cometary bodies also attests to this coagulation record. Coagulation likely plays an equally important role in the formation of other planetary systems. Some evidence for that can be found in the very large grain sizes implied by millimeter observations of dust disks around T Tauri stars. Likewise, a proper understanding of the β Pic phenomenon requires detailed knowledge of the structure and stability of the planetesimals responsible for the dust debris observed in the IR.

Various studies have been published over the years on clustering under astrophysically relevant conditions (Wright 1987; Meakin & Donn 1988; Ossenkopf 1993; among others). Generally, these adopted a ballistic trajectory approach without restructuring; i.e., a single grain (or a cluster) collides with a cluster on a random, straight-line trajectory whereby the incoming particle sticks at the point

of contact. In a few cases, a more sophisticated approach has been taken. For example, Meakin & Donn (1988) and Richardson (1995) allow the incoming grain/cluster to rotate until three points of contact are made. However, no real physics was involved, and the effects of material properties (binding energy, elasticity) and grain properties (velocity, radii) were not taken into account. Yet, this restructuring is of fundamental importance because it determines the mass-size relationship or equivalently the fractal dimension or porosity. This in turn determines the interaction with the gas, including the drag, and, hence, controls the whole growth and sedimentation process. In particular, ballistic particle-cluster aggregation (BPCA) leads to a (non)fractal dimension of 3 although this is reached only for aggregate sizes of the order of 1000 grains (Ossenkopf 1993). On the other hand, ballistic cluster-cluster aggregation (BCCA) leads to much smaller fractal dimensions (typically somewhat less than 2). A dimension of 2 or less implies that the drag force increases only slowly with aggregate size and the aggregates couple to the gas much better than more compact structures. A dimension larger than 2 leads to reduced coupling between gas and dust. Also the optical properties of dust aggregates are dependent upon their structure (see, e.g., Kozasa, Blum, & Mukai 1992).

Fortunately, the physics underlying coagulation has wide-ranging applications in the fields of friction, lubrication, surface deformation, materials elastic and plastic response characteristics, and atomic scale manipulation of surface structures. Driven by this fundamental interest, in recent years, our understanding of materials interaction on an atomic scale size has grown rapidly. From the experimental side, the development of the scanning tunneling and atomic force microscopes has allowed increasingly sophisticated studies of tip-substrate interactions on a nanometer size scale—the typical size of the contact areas of submicron-sized grains (for an overview, see Wiesendanger & Güntherodt 1993). On the theoretical side, the ever-increasing speed of supercomputers now allows routine numerical investigations of the microscopic interactions on an atom-by-atom basis (see, e.g., Landmann & Luedtke 1993). These studies have allowed researchers to probe in great detail the morphology, structure, and interaction of surfaces, including the microscopic response and deformation processes. It was demonstrated that many of the characteristic features of coagulation can be understood on the basis of continuum elastics (Johnson, Kendall, & Roberts 1971), which simplifies studies of coagulation of small grains considerably.

Drawing heavily from these studies, we have in recent years developed simple theoretical tools to describe the processes involved in the sticking and coagulation of small grains (Chokshi, Tielens, & Hollenbach 1993; Dominik & Tielens 1995, 1996). This allows us to develop a theoretical model for the stability and structure of collisional agglomerates as a function of the material parameters and the collisional history. In this way, we can analyze the mass-size relationship/fractal dimension/porosity of collisional agglomerates. This paper details this model. In § 2, we summarize the physics of the contact between two dust grains, concentrating on the energy dissipation due to elastic wave excitation driven by contact formation and due to the agglomerate restructuring driven by rolling and sliding motions. This energy dissipation is at the core of the model for sticking probability of colliding grains. Based upon this physical model for the interaction forces through contact areas, we present in § 3 the results of numerical calculations on particle-cluster and cluster-cluster collisions. These studies allow us to develop a recipe for calculating grain coagulation as a function of material parameters, velocity, and cluster size. This recipe is described in § 4. This section also presents an example calculation of the collisional agglomeration process in space.

2. PHYSICS OF THE CONTACT BETWEEN TWO DUST GRAINS

In order to study the coagulation process and collisions between aggregates more realistically, it is necessary to understand the physics of a contact between two dust grains. Here, we will concentrate on small stresses where continuum elastics applies. Large stresses can lead to plastic deformation or even shock waves. These have been discussed in an astrophysical context by Chokshi et al. (1993), Tielens et al. (1994), and Jones et al. (1996).

Two grains can make contact if there is an attractive force between them. The lower limit for such a force is, of course, the van der Waals attraction, but other, stronger forces such as dipole-dipole interaction between ices or metallic binding may be involved for some materials. In principle, the grains may also be charged, giving rise to either attractive or repulsive forces. However, in the ISM, grain charging will be dominated by gas-grain collisions and hence couples to the thermal bath. In contrast, for grains larger that a critical size $a_{\rm cr}$, grain-grain collisions tap the turbulence of molecular clouds (Weidenschilling & Ruzmaikina 1994; Markiewicz, Mizuno, & Völk 1991). For dark cloud conditions, this critical size is about 250 Å. Since the turbulent energy dominates by many orders of magnitude the thermal energy of molecular clouds, Coulombic forces have little influence on the coagulation process (see Chokshi et al. 1993).

Attractive forces pull the two grains together, forming a contact area where the grain surfaces react with deformation (are being pressed flat) until the elastic repulsion force balances the attractive forces. This kind of contact is from a theoretical point of view an extension of the classical work of Hertz who, following Newton's famous experiments, studied the deformation of bodies in contacts without adhesion (Hertz 1896). The effects of adhesion on the deformation process have been studied in great detail in material sciences in connection to friction between surfaces (see, for example, Singer & Pollock 1992 and references therein). In recent years, the development of the atomic force microscope has given new momentum to this field (see, e.g., Wiesendanger & Güntherodt 1993 and references therein). The first consistent theoretical descriptions are due to Johnson et al. (1971) and Sperling (1964). In this JKRS theory, the forces between the bodies in contact are assumed to be pure contact forces; i.e., the grains feel the mutual attraction only when they are actually in contact and only in the area where there is contact. The geometry of such a contact is shown in Figure 1. In the absence of external forces, the equilibrium contact radius, a_0, is given by

$$a_0 = \frac{9\pi\gamma R^2}{\mathscr{E}^\star}\,. \tag{1}$$

The radii R_1, R_2 of the dust grains in contact enter into

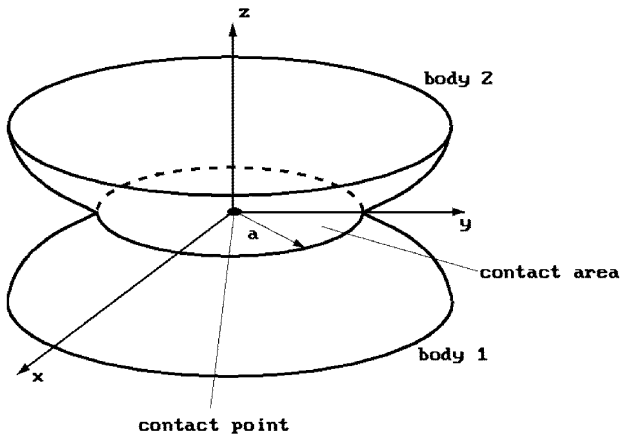

FIG. 1.—Contact geometry: Two grains make contact over a finite circular area with radius a. The size of the area is controlled by the competition between attractive (van der Waals, dipole, etc.) forces and repulsive elastic forces.

this expression as the reduced radius R ($R^{-1} = R_1^{-1} + R_2^{-1}$). The attractive forces are described by the surface energy γ of the material. For different materials, $\gamma = \gamma_1 + \gamma_2 - 2\gamma_{12}$, where γ_{12} is the interface energy. For like materials, $\gamma_1 = \gamma_2$ and $\gamma_{12} = 0$. The elastic forces enter via the material constant $\mathscr{E}^*$, which is given by $(\mathscr{E}^*)^{-1} = (1 - \nu_1^2)/\mathscr{E}_1 + (1 - \nu_2^2)/\mathscr{E}_2$ with ν_i and $\mathscr{E}_i$ the Poisson's ratio and Young's modulus, respectively, of grain i.

The contact between two grains has a total of 6 degrees of freedom as indicated in Figure 2. There is 1 vertical degree of freedom, 2 for both rolling and sliding in the plane of the contact, and 1 for a relative spinning motion of the two grains about the axis connecting the centers of the two spheres (for an excellent discussion of the geometrical aspects, see Johnson 1989). Every relative motion of the grains can be decomposed into these six components. The vertical degree of freedom (Fig. 2*a*) covers motions along the axis connecting the centers of the two grains, i.e., when the grains move closer together or farther apart. The rolling degree of freedom (Fig. 2*b*) describes rolling of the two grains over each other. It is a motion with constant distance and without sliding of the surfaces. The center of the contact circle (*contact point*) moves with equal speed in the same direction over the two grain surfaces. The sliding degree of freedom (Fig. 2*c*) covers a relative motion of the grains without rotation and with constant distance. The grain surfaces slide over each other, and the contact point moves in the opposite direction over both surfaces. Finally, the spinning degree of freedom covers a differential rotation of the grains about the axis connecting the centers of the spheres. The contact point does not move, but the surfaces in contact slide relative to each other with a velocity proportional to the distance from the contact point.

When external forces are applied to the grains (e.g., inertial forces in a collision), the forces will be transmitted from one grain to the other via stresses in the contact region. The stresses lead to deformation of the grains near the contact region. Generally, we may expect that for small forces, there is an elastic reaction of the contact: when the external forces are released, the deformation is reversed and the original state recovered. However, when the forces become larger than some limit, irreversible changes will occur. Pulling grains apart with a small force will only reduce the contact area, while pulling harder will eventually break the contact. Similarly, a small tangential force will only deform the grains near the contact, but a larger force will lead to rolling or sliding and move the contact around. These irreversible processes are connected with the dissipation of energy. Their understanding is essential for the physics of coagulation as they ultimately determine structure and stability of dust aggregates.

The detailed physics involved in the different degrees of freedom have recently been discussed in a series of papers (Chokshi et al. 1993, hereafter Paper I; Dominik & Tielens 1995, hereafter Paper II; and Dominik & Tielens 1996,

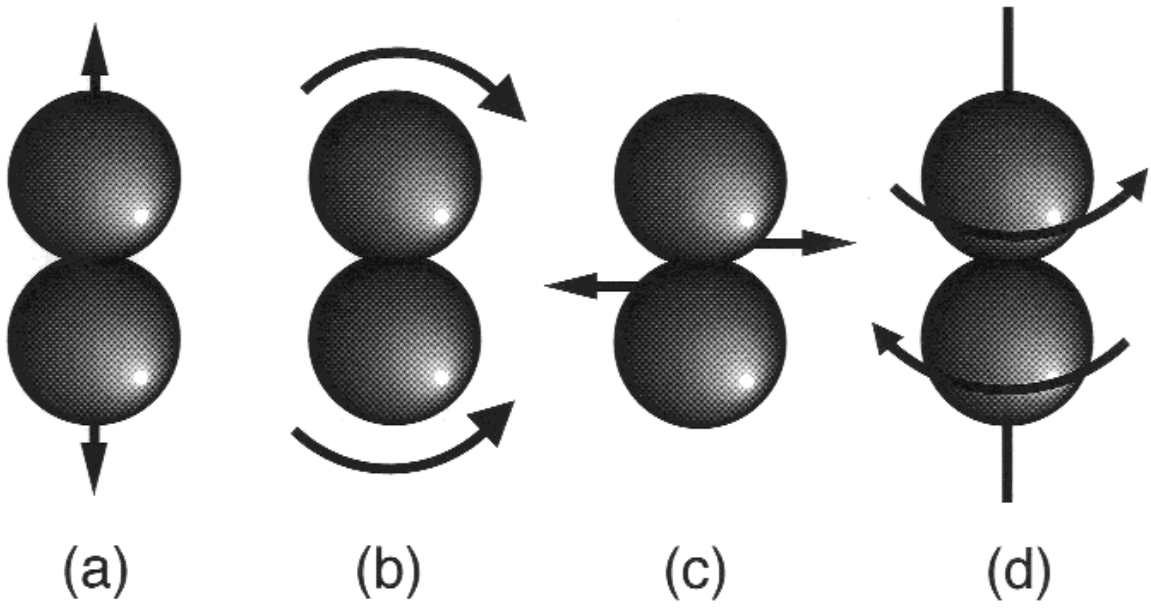

FIG. 2.—The different degrees of freedom of a contact between two particles: (*a*) vertical (pull-off), (*b*) tangential (rolling), (*c*) tangential (sliding), (*d*) torsional (spinning).

hereafter Paper III). In the remainder of this section, we will review the results.

2.1. *The Vertical Degree of Freedom*

The first degree of freedom shown in Figure 2*a* is the vertical degree. Forces that act only in this direction must either pull the grains apart or push them together along the line connecting the centers of the two grains. This is in particular the case in head-on collisions of nonrotating spheres.

Chokshi et al. (Paper I) have discussed this in detail. They based their discussion on the JKRS solution of the adhesive contact between two elastic spheres. As this is the *static* solution of the contact problem, it is important to realize that the contact can in fact be treated as quasi-static in a dynamic process such as a collision of two grains. Chokshi et al. showed that the collision times are generally much longer than the sound travel times in the grains. Since the adjustment of the contact to its equilibrium point happens on a sound travel time (except for viscoelastic materials like gel; see the discussion in Kendall 1980), the quasi-static assumption is actually well justified.

Let us first consider two grains that have already been in contact for a long time, so that all vibrational energy in the vertical direction has been dissipated. The grains are at rest relative to each other, and the radius of the contact area equals the equilibrium value a_0. If we now pull the grains apart, the contact radius changes according to

$$a = \left\{\left(\frac{3R}{4\mathscr{E}^*}\right)\left[F + 6\pi\gamma R + \sqrt{(6\pi\gamma R)^2 + 12\pi\gamma RF}\right]\right\}^{1/3}, \tag{2}$$

where F is the applied force (Paper I).

If we want to break the contact by pulling the grains apart, a certain amount of energy has to be provided. Owing to the attractive forces in the contact area, the grain surfaces stay in contact even if the separation of the grain centers becomes larger than the sum of the grain radii. A neck of material is pulled out of the grains as is indicated (greatly exaggerated) in Figure 3*a*. At a critical pulling force

$$F_c = 3\pi\gamma R\,, \tag{3}$$

the surfaces separate suddenly, and the elastic energy stored in the neck is transformed into elastic wave and slowly dissipated. The amount of this energy follows directly from

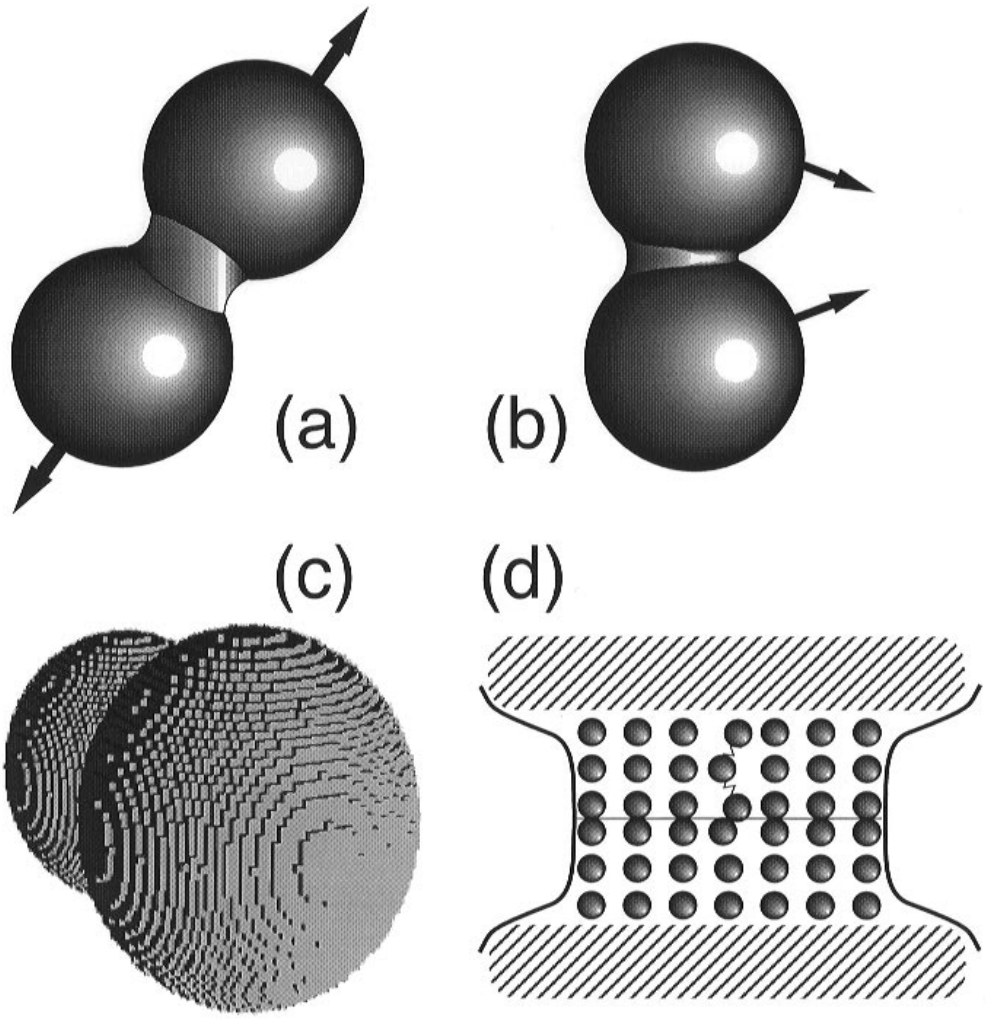

FIG. 3.—Four different major processes contributing to energy dissipation in contact dynamics of (sub)micron-sized spheres: (*a*) neck formation during pull-off; (*b*) lagging of the contact area during rolling; (*c*) surface roughness, lower limit given by atomic structure of the surfaces; (*d*) energy dissipation due to jump-wise sliding motion of individual atoms. The sketches are not to scale. All processes have been greatly exaggerated.

the JKRS theory and is given by

$$E_{\rm JKRS} \simeq 0.09 F_c \delta_c \tag{4}$$

$$\simeq 2.1 \times \frac{\gamma^{5/3} R^{4/3}}{\mathscr{E}^*} . \tag{5}$$

The situation is slightly different in a dynamic situation such as a collision. For now, we restrict ourselves to a head-on collision so that tangential components of the contact forces can be neglected. During a head-on collision, the grains approach each other along a line connecting the centers of the two spheres. Before contact, they do not feel any mutual forces, since we consider contact forces only. Once the grain surfaces touch, the first forces are transmitted. On a sound crossing time of the contact area, the contact point grows to a contact area with a size given by the static theory. The attractive interaction energy across this newly formed contact quickly accelerates the grains toward each other. As the grains continue to move, the contact area grows steadily. When the contact radius reaches the equilibrium value a_0, the grains are no longer accelerated toward each other but still move owing to their inertia. The overall force in the contact area now becomes repulsive, decelerates the motion, and eventually turns the direction of motion around pushing the grains apart. The important point is now that the grain surfaces do not separate again at the same distance at which they first made contact. Instead, as discussed above, a neck of material is pulled out of both grains (Fig. 3*a*). The grains separate only when they reach a critical separation δ_c (see Paper I for details). Again, the pulling out of the neck requires energy. If the initial kinetic collision energy was not large enough to pull out this neck, the grains do not separate but stick together. Thus, it is this asymmetry between contact making and contact breaking that actually enables grains to stick together.

Chokshi et al. also looked at the excitation of elastic waves in the colliding grains and showed that this actually requires an amount of energy 4 times larger than the pulling out of the neck. Taking both effects into account, it was shown that two grains will stick when the kinetic collision energy does not exceed the critical value

$$E_{\rm stick} = 0.4 \times F_c \delta_c \tag{6}$$

$$\approx 9.6 \times \frac{\gamma^{5/3} R^{4/3}}{\mathscr{E}^*} . \tag{7}$$

In that case, the initial kinetic energy plus the net interaction energy (i.e., attractive energy − elastic repulsion energy) will be converted into thermal phonon energy on a timescale of $\approx 10^{-5}$ s and eventually radiated away (Paper I). This leaves the two grains trapped in their potential well with a net energy of $\approx 1.5 F_c \delta_c$. In order to separate the grains again, this energy has to be supplied. Moreover, the breakup process will excite elastic waves in much the same way as a collision. Since the forces are the same, the energy required to excite these waves is given by the difference between equation (5) and (7), and the total energy required to break an existing contact is given by

$$E_{\rm break} = 1.8 \times F_c \delta_c$$

$$\approx 43 \times \frac{\gamma^{5/3} R^{4/3}}{\mathscr{E}^*} . \tag{8}$$

Here and later, we give the critical values as energies, as this is the more fundamental quantity. However, sometimes it easier to think in terms of a critical velocity that is equivalent to the critical energies. The corresponding critical velocity is given by

$$v_{\rm stick} = \sqrt{\frac{2}{\mu} E_{\rm stick}} , \tag{9}$$

where $\mu = m_1 m_2/(m_1 + m_2)$ is the reduced mass of the two colliding grains. To compute critical velocities, we therefore need to specify the masses or sizes of both grains, not just the reduced values. For two identical spheres, each of them with a radius $R_1 = 2R$, the critical velocity for sticking is given by[1]

$$v_{\rm stick} = 1.07 \frac{\gamma^{5/6}}{\mathscr{E}^* R^{5/6} \rho^{1/2}} , \tag{10}$$

where ρ is the specific density of the grain material.

It is easy to see that, although the critical energy *increases* for increasing grain sizes (eq. [7]), the critical velocity *decreases* since the grain mass is a steeper function of R than the critical energy. This is also true for all critical energies discussed in the following sections and should be kept in mind. We have plotted the critical sticking energy and the critical energy for breaking a contact for the case of silicate grains in Figure 4*a*. Both energies show the same power-law dependence upon the reduced radius R. The critical energy for sticking is smaller by a constant factor of ≈ 4.75 than the energy required to break an existing contact (see eqs. [7] and [8]).

2.2. *The Tangential Degrees of Freedom*

In realistic situations, head-on collisions of nonrotating spheres will be the exception. Therefore, in almost any collision, there will be motions of the grains in a direction perpendicular to the axis connecting the grain centers. The tangential forces involved may lead to rolling, sliding, and twisting of the contact, each of which will be discussed in turn.

2.2.1. *Rolling*

The rolling degree of freedom is shown in Figure 2*b*. In the rolling motion, new contact is made at one side of the contact area while old contact is lost at the opposite side. Any resistance to this type of motion is called *rolling friction*. To understand the response of a contact to this kind of motion, the sources of rolling friction need to be studied.

The classical sources of rolling friction such as microslip at the interface, inelastic or viscoelastic deformation of the involved materials, and large surface irregularities turn out not to be important in the case of the (sub)micron particle sizes that we need to consider in the astrophysical context. However, for such small particles, it becomes important that the surfaces are not smooth at all scales but are made of atoms. When two grains roll over each other, new contact between atoms at the leading edge needs to be made, and contact between atoms at the trailing edge is lost. For ideal spheres and in a quasi-static approach, the contact area would always be symmetrical around the axis connecting the centers of the spheres. However, since the

[1] Note that this result is different from eq. (28) in Paper I. The result in Paper I is erroneous.

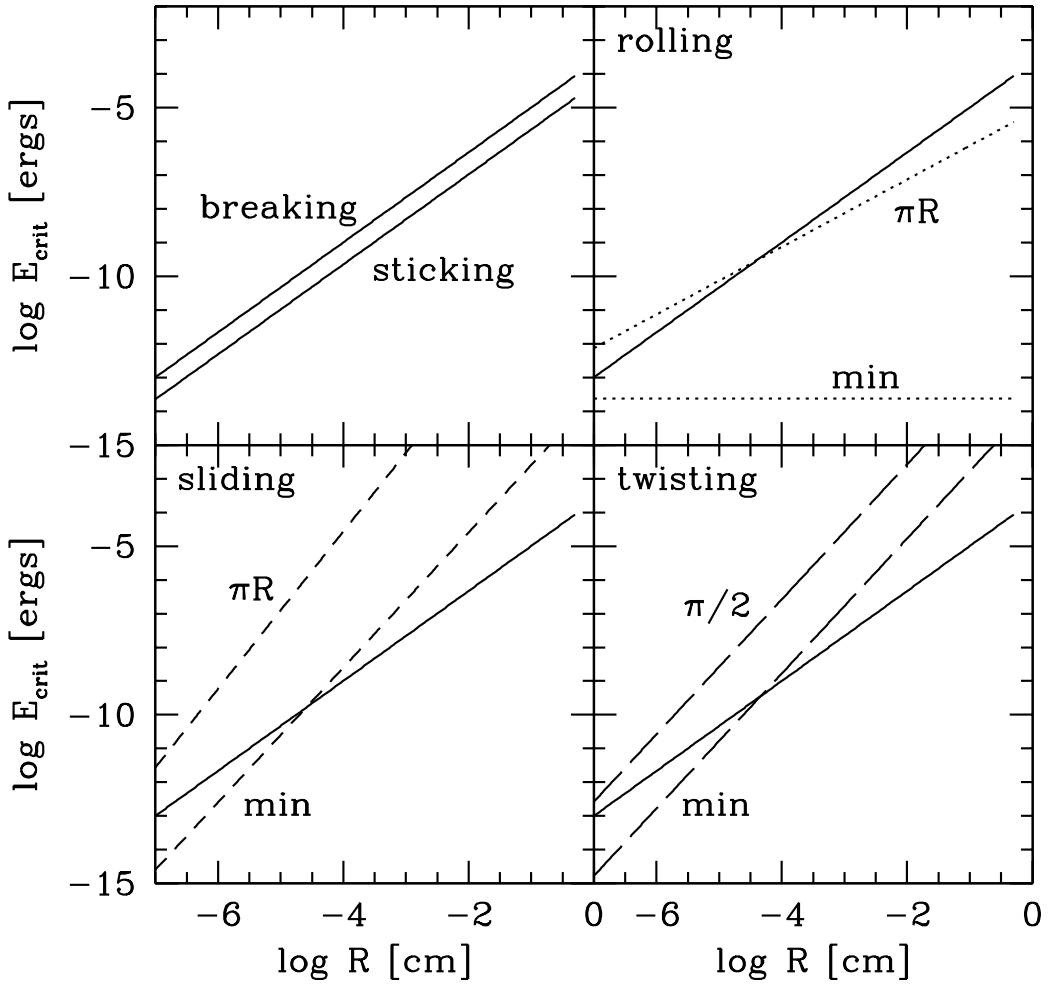

FIG. 4.—Energy required to restructure an aggregate by moving a single contact. Silicate material properties were chosen for this example. The results are plotted as a function of reduced particle radius R. Diagram (*a*) shows the critical energies for sticking and breaking. Diagrams (*b*), (*c*), and (*d*) show the respective energies for the restructuring processes rolling, sliding, and twisting. The solid line always gives the breakup energy as a reference. The lower broken lines show the minimum energy required to leave the elastic limit and start moving the contact at all. The upper lines show the energy required to move the contact between identical spheres by one-quarter of the particle radius.

surfaces are made of atoms, new contacts can be made only in steps of at least one atom, and old contact can only be lost in steps as well. Thus, when the grains start to roll over each other, the contact area does not move at first but stays fixed. This leads to an *asymmetric* pressure distribution that is connected with a torque force opposing the rolling motion:

$$M = 4F_c\left(\frac{a}{a_0}\right)^{3/2}\xi\,, \tag{11}$$

where ξ is the linear distance the contact area is lagging behind (Paper II).

For small motions around the equilibrium point, the contact area will not move at all. The torque given in equation (11) is then linearly proportional to the displacement—the contact behaves like a spring. When the rolling motion exceeds a certain critical shift, $\xi_{\rm crit}$, the contact area starts to move and energy is dissipated. Thus, just as in the vertical degree of freedom, there is a limited regime in which the contact reacts elastically to forces. Beyond this limited range, inelastic behavior occurs.

The torque needed to start irreversible rolling is (see Paper II)

$$M_{y,\rm crit} = M_y(\xi_{\rm crit}) = 4F_c\left(\frac{a}{a_0}\right)^{3/2}\xi_{\rm crit}\,. \tag{12}$$

Its dependence upon the size of the contact area [the $(a/a_0)^{3/2}$ factor] is weak and can safely be omitted for analytical discussions. However, we take it fully into account in the numerical calculations.

The energy associated with starting rolling is

$$e_{\rm roll} = 2F_c\,\frac{\xi_{\rm crit}^2}{R} \tag{13}$$

$$= 6\pi\gamma\xi_{\rm crit}^2\,, \tag{14}$$

which is also the energy dissipated on average during rolling over a distance $\xi_{\rm crit}$. It is independent of the reduced radius R. Since the motion of the contact area is limited by the size of an atom, we will assume that $\xi_{\rm crit}$ is equal to 1 Å unless otherwise mentioned.

Later in this paper, we will study the rearrangement of aggregates. For this process, the energy required to start

rolling (to roll a small distance $\xi_{\rm crit}$) is only one of the important quantities. In order to restructure visibly a part of an aggregate, rolling would have to proceed over a distance typical for the size of the individual particles in the aggregate. We therefore define another critical quantity $E_{\rm roll}$, which is the energy required to roll a distance πR. In the contact of two equal spheres, this would imply a movement of 90° of the distance vector between the two grains. For rolling, we find

$$E_{\rm roll} = e_{\rm roll} \frac{\pi R}{\xi_{\rm crit}} = 6\pi^2 \gamma R \xi_{\rm crit} . \quad (15)$$

The two critical energies for rolling have been plotted for silicate material properties in Figure 4*b*. For reference, the solid line shows the critical energy for breaking an existing contact, taken from Figure 4*a*. The energy required to initiate rolling is independent of the reduced particle radius R (see eq. [13]) and is for all sizes much smaller than the energy required to break a contact. This already indicates that it should easily be possible to start some rolling in an aggregate without destroying it. However, the energy required to roll a "visible" distance is similar to the breakup energy. Therefore, it will be rather difficult to roll over large distances in an aggregate without breaking it at the same time. This is not surprising since the stresses and forces involved in rolling and breaking are very similar. Comparing equations (8) and (15), we see that the ratio of the energies for rolling and breakup is $\xi_{\rm crit}/\delta_c$. Because the compression of the contact area, δ_c, is of the order of a few interatomic distances for submicron-sized grains (i.e., $\xi_{\rm crit} \approx \delta_c$), the energies are similar for rolling distances of the order of R.

It should be mentioned that there are two basic factors that could inhibit rolling at the energies calculated above and increase the critical energies. The considerations in Paper II are based on the assumption that at least one of the surfaces in contact is "round" so that the contact really is of the nature of the JKRS solution. If both surfaces in contact are flat over the contact region (imagine a couple of cubes in contact), rolling would be more difficult, since one would have to break the contact on the entire contact region before any motion would be possible. This would make the energy required to initiate rolling already similar to the breakup energy. The relatively low resistance to rolling found above is based on the fact that only the contact near the rim of the contact region needs to be broken and remade. A second mechanism to inhibit rolling is the accretion of additional material onto the aggregates *after* contact formation. This material would form an unstrained belt around the contact to which the above description would again not apply. In order to start rolling, either this new material has to be broken away or the original contact needs to be broken in order to roll *over* the accreted material. This process might be of some relevance to dark clouds where at low temperatures ices can be accreted. We will, however, ignore it here.

2.2.2. *Sliding*

The sliding degree of freedom is shown in Figure 2*c*. It is a motion where atoms in the different surfaces move (slide) over each other instead of only approaching and receding from the other surface as it is the case for rolling. Any resistance to this type of motion is called *sliding friction*. To understand the response of a contact to this kind of motion, the sources of sliding friction need to be studied.

The classical source of sliding friction is material wear. For macroscopic applications, surface irregularities are pressed flat and surface grooves are carved out during sliding, and the engineering literature on (sliding) friction is mainly concerned with these processes. However, again in the situation relevant for coagulation of (sub)micron-sized grains, this is different. For one, at microscopic size scales, surface irregularities are less relevant, and yield stresses are very high. Moreover, the grains are held together only by their mutual attraction instead of large external forces, and hence, the pressures in the contact region are generally too small for the above named processes to be important.

Still, there are two sources of sliding friction that are relevant to our case:

1. Surface "roughness" on atomic scale—i.e., steps in the surface grid of the grain material. Compression of this surface structure will lead to friction.
2. Energy losses on atomic scales owing to instabilities in the sliding motion of individual atoms. These losses can even be present when two perfectly smooth surfaces slide over each other.

We will first estimate the friction forces associated with these two processes and subsequently calculate the energy dissipation associated with those forces.

It is fairly simple to estimate the contribution of steps in the surface grids to sliding friction. Such steps will always be present on roughly spherical particles. The number of steps on a given circumference of a sphere can be estimated to be $2R/b$, where R is the radius of the sphere and b is the interatomic distance (Paper III). When two steps on the surfaces meet, they have to be pressed flat. The energy required to do this can be calculated in analogy with Frenkel's calculation of the strength of ideal crystals (see, e.g., Kittel 1976). The friction force due to this mechanism is given by (Paper III)

$$F_{\rm fric}^{\rm steps} = \frac{G}{2\pi} \pi a^2 , \quad (16)$$

where $G = 1/(G_1^{-1} + G_2^{-1})$ is the reduced shear modulus of the grain materials, and a is again the radius of the contact area. We may rewrite this as

$$F_{\rm fric}^{\rm steps} = 0.39 \frac{(1-\nu^2)^{2/3}}{1+\nu} \left(\frac{E}{\gamma}\right)^{1/3} R^{1/3} F_c \approx 3 \cdots 50 \left(\frac{R}{10^{-5}\ {\rm cm}}\right)^{1/3} F_c \quad (17)$$

with the numerical factor ranging from 3 to 50 for different materials. Thus, sliding friction by this process is usually larger than the pull-off force F_c.

The second mechanism providing sliding friction is the dissipation of energy on atomic scales due to "instabilities" in the sliding motion of individual atoms (Tománek 1993; McClelland 1989). When an atom is sliding over a step-free surface, there are two forces acting on the atom. It interacts with other atoms of the body of which it is a part (henceforth A-A interaction) and also with the atoms of the surface upon which it is sliding (A-B interaction). If the interaction with the other surface is weak compared to the binding forces, that surface is merely a weak disturbance

and the sliding motion will be smooth and without energy dissipation unless the sliding atom is pressed heavily onto the surface.

However, if the A-B interaction is of the same magnitude as the A-A interaction, the motion of the atom is strongly influenced by the presence of the surface even in the absence of strong *external* pressure (i.e., forces applied to the grains in contact). During sliding, the atom may get "caught" in a potential well in the surface and may be released only when the rest of the sliding body has moved on for more than a grid constant. The atom will then jump to the new equilibrium position, and the energy stored in the strained bonds will be partially dissipated.

This second source of sliding friction is therefore active only when the forces between the atoms of the two surfaces are of (at least) the same magnitude as the forces within the surface. This is the case for ices and for metals, since the interaction through the contact is provided by the same mechanism (dipole forces, hydrogen bonding, metallic bonding) as the binding forces of the particle bulk material. However, grains made of quartz or graphite are mutually attracted only by van der Waals forces, which are much weaker than the chemical Si—O and C—C bonds. The second source of sliding friction is absent in these materials.

This mechanism has been a matter of great interest in the field of tribology recently (see, e.g., Singer & Pollock 1992 and references therein). However, calculations of the forces involved and energies lost are still limited to classical calculations of the interatomic forces. Quantum mechanical theories are not available. In Paper III, we have used a similar classical calculation to determine the friction force for astrophysically relevant materials. There we also give the general solution that integrates the friction terms over only the central part of the contact area where the pressure exceeds a critical pressure $p_{\rm crit}$. Here, we restrict ourselves to two limiting cases. For materials where the A-B interaction is much weaker than the A-A interaction (graphite, quartz, organic mantles), the sliding friction due to the instability process is zero. For the materials ice and iron, it can be assumed with good accuracy that the mechanism is active over almost the entire contact area. Then the sliding friction is given by

$$F_{\rm fric}^{\rm slide} = \frac{1}{3} F - \frac{\pi a^2}{3} p_{\rm crit} , \tag{18}$$

where F is the vertical pressure. The critical pressure is a material constant and is given by

$$p_{\rm crit} = \frac{2.67}{\pi} \frac{b^3}{\sigma^3} G - \frac{24.72}{\pi} \frac{b^4}{\sigma^5} \gamma , \tag{19}$$

where b is the interatomic distance in the grain material and $\sqrt[6]{2}\sigma$ is the equilibrium distance in the pair-potential model for the A-B interaction. For details, see Paper III.

The actual sliding friction force for a material will be given by the sum of the two contributions from equations (16) and (18):

$$F_{\rm fric} = \frac{G}{2\pi} \pi a^2 + \begin{cases} 0 & \text{silicate, graphite, etc.} \\ \frac{1}{3} F - \frac{\pi a^2}{3} p_{\rm crit} & \text{ice, metal.} \end{cases} \tag{20}$$

The force given by equation (20) is the force that will oppose sliding. When a tangential force F_x is applied to the contact that is smaller than $F_{\rm fric}$, the material near the contact will be strained and the grains will be displaced relative to each other by an amount of

$$\delta_x = \frac{1}{8aG^*} F_x , \tag{21}$$

where $1/G^* = [(2 - \nu_1)/G_1 + (2 - \nu_2)/G_2]$ (see, e.g., Johnson 1989). Again, this is a springlike behavior. Force and displacement are proportional to each other. As with pull-off and rolling, there is a small region of force and displacement where the contact reacts elastically. Only when the displacement becomes larger than $\delta_x^c = \delta_x(F_{\rm fric})$ do the grains start sliding over each other. The energy associated with straining the contact from the equilibrium point to δ_x^c is given by $\delta_x^c F_{\rm fric}/2$. We use this to define the critical energy required to start sliding by

$$e_{\rm slide} = \frac{1}{16aG^*} F_{\rm fric}^2 , \tag{22}$$

which is also the energy dissipated on average during sliding over a distance δ_x^c. In analogy to the rolling degree of freedom, we also define an energy $E_{\rm slide}$, which is the energy required to slide over a distance πR and is given by

$$E_{\rm slide} = e_{\rm slide} \frac{\pi R}{\delta_x^c} \tag{23}$$

$$= \frac{1}{2} \pi R F_{\rm fric} . \tag{24}$$

The two critical energies for sliding have been plotted for silicate material properties in Figure 4*c*. The minimum energy required to start sliding is already very similar to the energy that is sufficient to break a contact. This was to be expected already from the result in equation (17). For grain materials such as ice or metal, the friction is even stronger than that because the second mechanism works here as well. The energy required to slide a "visible" distance is much greater than the breakup energy for all realistic particle sizes. This clearly shows that the sliding process will be much less relevant to restructuring aggregates than the rolling process. When in a collision the energies concentrated in individual contacts are big enough to start sliding, the aggregate will most certainly break into pieces rather than be restructured.

2.2.3. *Twisting*

In twisting, both grains in contact rotate around the axis connecting the centers of the spheres with different angular velocities (see Fig. 2*d*). The surfaces in the contact region must slide over each other to allow for such a motion. Therefore, the physical mechanisms providing friction are the same as discussed in the previous section. In Paper III, we have shown the torque due to surface steps is given by

$$M_z^{\rm steps} = \frac{Ga^3}{3\pi} . \tag{25}$$

For the torque due to "instabilities" in the motion of atoms, we restrict ourselves to the limiting case in which the entire contact region contributes to the friction. In this case (a good approximation for ice and metal grains), this torque

is given by

$$M_z^{\rm slide} = \frac{\pi}{3} F_c a_0 \left[\frac{3}{4} \left(\frac{a}{a_0} \right)^4 - \left(\frac{a}{a_0} \right)^{5/2} \right] - \frac{2}{9} \pi a^3 p_{\rm crit} . \quad (26)$$

For silicate and graphite grains, the contribution of this process to friction is zero as in the sliding degree of freedom. The total torque that can be sustained without starting to twist is given by

$$M_z^{\rm crit} = \frac{Ga^3}{3\pi} + \begin{cases} 0 & \text{silicate, graphite, etc.} \\ M_z^{\rm slide} & \text{ice, metal.} \end{cases} \quad (27)$$

Before onset of twisting, there is again a linear relation between angular displacement $\delta_{\alpha z}$ and the torque exerted by the strained material in the contact region. That relation is (see, e.g., Johnson 1989)

$$\delta_{\alpha z} = \frac{3}{16Ga^3} M_z . \quad (28)$$

The critical angular displacement is reached when the torque M_z is equal to the critical torque $M_z^{\rm crit}$. Since the torque varies linearly with the displacement, the energy associated with this is $M_z^{\rm crit} \delta_{\alpha z}/2$. We use this to define the critical energy required to start twisting

$$e_{\rm twist} = \frac{3}{32Ga^3} (M_z^{\rm crit})^2 . \quad (29)$$

The second critical energy $E_{\rm twist}$ is defined to be the energy required to twist over an angle of $\pi/2$ and is given by

$$E_{\rm twist} = \frac{\pi}{2} M_z^{\rm crit} . \quad (30)$$

The two critical energies for twisting have been plotted for silicate material properties in Figure 4*d*. Since the physical mechanisms providing for friction in this case are the same as in the sliding degree of freedom, the critical energies are very similar in both cases. This is in particular true for the critical energy required to leave the elastic domain and start sliding or twisting. However, the critical energy for twisting a "visible" amount is 1 order of magnitude smaller than the same quantity for sliding because twisting 90° corresponds to a linear distance of only $\pi a/2$, while sliding 90° covers a much larger distance (πR). Since the radius of the contact area is much smaller than the grain radius, it is actually easier to restructure an aggregate "visibly" by twisting than it is by sliding. However, the energy $E_{\rm twist}$ is still considerably larger than the breakup energy for all realistic particle sizes. Therefore, the conclusions drawn for the relevance of sliding for restructuring grains aggregates basically still hold for twisting.

2.3. *Energy Domains for the Different Restructuring Processes*

All processes discussed are material dependent. The adopted material constants are listed in Table 1 for five materials of astrophysical interest: quartz (as prototype for astrophysical silicate), graphite, polystyrene (as an analog of organic mantle material), ice, and iron. The values adopted have been justified in detail in Paper I.

The different restructuring processes discussed above each define intervals in energy for which the respective process is (*a*) impossible, (*b*) possible but without "visible" effect, and (*c*) possible with a visible effect. The critical energies all have a power-law dependence upon the reduced grain radius R; they are straight lines in a log R–log $E_{\rm crit}$ diagram (see Fig. 4). Therefore, they may be written as

$$\log E_{\rm crit} = A \log R + B \quad (31)$$

with material-dependent constants A and B (Table 2). All the coefficients can be derived from the equations given in Papers I, II, and III for any other material under consideration.

The discussion in the previous section showed that rolling is the main candidate for successful aggregate restructuring processes and that twisting may come into play for small grains. However, sliding may be neglected in the first approximation (but see § 3.6). Thus, for a simplified discussion of the different energy domains, it is sufficient to look at rolling, breakup, and twisting alone. In Figure 5 we show domains in the reduced radius-energy diagram where the different processes are possible and effective. The plot shows these domains for the five different materials. The full horizontal line in all plots shows the critical energy for onset of any restructuring mechanism. Except for very small grains, this line is always given by the rolling process. In the dotted region above this line, rolling is in principle possible, when the energy marked on the ordinate is available to the rolling degree of freedom of a single contact. For the materials quartz, polystyrene, and graphite, the diagrams also show a striped region at small values for the reduced particle radius R. In these areas, twisting and sometimes sliding are also possible. However, in both regions, the energy is not large enough to produce a large visible effect by moving a contact over a distance πR. Examining Figure 5, we conclude that larger grains can roll on a larger fraction of the energy parameter space. Recall, however, that in velocity space, restructuring is actually more difficult for

TABLE 1

MATERIAL PARAMETERS

Material	γ[a] (ergs cm^{-2})	$\mathscr{E}$ (dyn cm^{-2})	G (dyn cm^{-2})	ν	ρ (g cm^{-3})	σ (Å)	b (Å)	References
Quartz	25[b]	5.4(11)	2.3(11)	0.17	2.6	3.44	1.84	1, 2, 3
Polystyrene.....	12	3.4(10)	2.1(11)	0.5	1.04	3.00	2.00	2, 4
Graphite.....	75	1.0(11)	3.8(10)	0.32	2.2	3.40	1.54	3, 5, 6
Iron	3000	2.1(12)	8.3(11)	0.27	7.7	2.24	2.24	2, 3, 7
Ice.....	370[c]	7.0(10)	2.8(10)	0.25	1.0	3.36	3.36	2, 3

[a] Surface energy per surface.
[b] Measured for micron-sized particles.
[c] Estimated from H-bonding,

REFERENCES.—(1) Kendall, Alford, & Birchall 1987; (2) Physics Vademecum (Anderson 1981); (3) Israelachvili 1992; (4) Kendall & Padget 1987; (5) Brocklehurst 1977; (6) Zisman 1963; (7) Easterling & Thölen 1972.

TABLE 2

COEFFICIENTS FOR CRITICAL ENERGIES

A. CRITICAL ENERGY PER CONTACT FOR ONSET OF RESTRUCTURING[a]

PROCESS	a_{crit}	b_{crit}				
		Quartz	Polystyrene	Graphite	Iron	Ice
Rolling.....	0	−13.63	−13.95	−13.15	−11.55	−12.46
Sliding	2	−0.60	0.22	−0.17	4.04	4.15
Twisting	2	−0.77	0.04	−0.34	3.89	4.00

B. CRITICAL ENERGY PER CONTACT FOR VISIBLE RESTRUCTURING[b]

PROCESS	A_{crit}	B_{crit}				
		Quartz	Polystyrene	Graphite	Iron	Ice
Sticking.....	4/3	−4.32	−4.12	−3.06	−1.26	−1.78
Breaking.....	4/3	−3.66	−3.47	−2.40	−0.60	−1.13
Rolling.....	1	−5.13	−5.45	−4.65	−3.05	−3.96
Sliding	7/3	4.77	5.33	4.81	7.62	7.04
Twisting	2	1.43	2.24	1.86	4.78	4.38

[a] $\log e_{crit} = a \log R + b$ with R and e_{crit} in units of cm and ergs.
[b] $\log E_{crit} = A \log R + B$ with R and E_{crit} in units of cm and ergs.

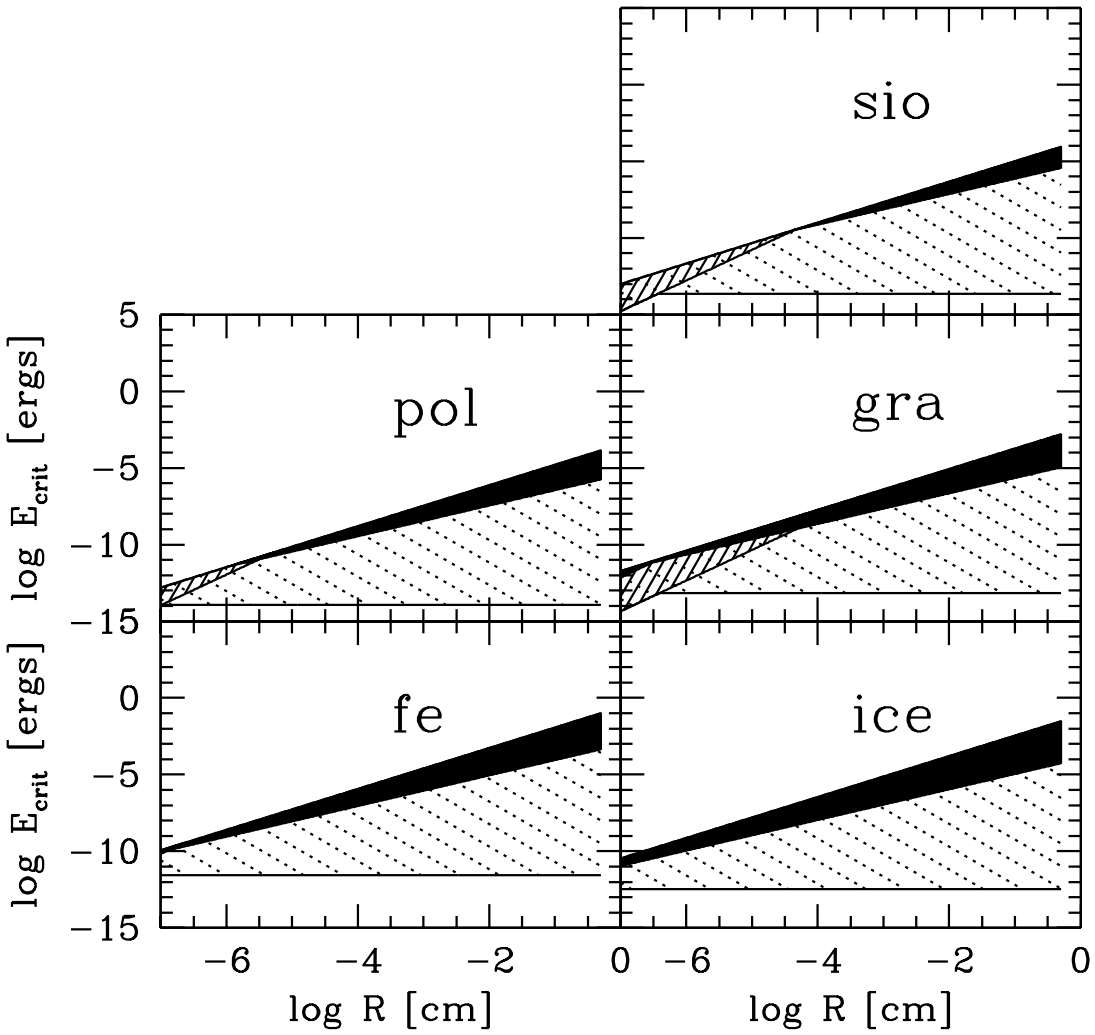

FIG. 5.—Restructuring domains as a function of energy per contact and reduced particle radius for different materials. In the region below the shaded areas, no restructuring can happen. Within the dotted region, rolling is possible. The striped areas mark a region in which sliding and/or twisting become possible. The solid regions mark energies high enough to produce large amounts of rolling (one-quarter of the circumference of the grains). Above the shaded regions, energies are sufficient to break the contact.

large grains (see eq. [9]). Visible restructuring is possible only in the solid filled area. This area is limited at the lower side by the critical energy for "visible" rolling effects. The upper border of the that region is given by the breakup energy: If more energy is concentrated in a single contact, the energy is sufficient to break the contact. As the different degrees of freedom are well coupled, energy originally concentrated in, say, the rolling degree of freedom will be redistributed into the other degrees as well. Thus, it is not likely that restructuring by rolling will work with an energy higher than about the breakup energy concentrated in a single contact. Therefore, the regime in which large restructuring effects are possible by putting energy into a single contact is limited to a rather narrow wedge in the log R–log E diagram.

Thus, we conclude that restructuring on a large scale has to rely on processes, where the energy to move a contact over a large distance is not transferred into the contact at once, but slowly, at the same rate as the energy is dissipated by the restructuring process. To use an analogy, aggregates are not compacted by shooting a bullet into them but rather by pressing them slowly and continuously. We will discuss the way this can be achieved in interstellar space when we discuss model calculations in the following sections.

3. COLLISIONS OF GRAINS AND AGGREGATES

With a quantitative description of the forces transmitted through contacts, it is now possible to carry out model calculation in much greater detail than has been possible before. Grain coagulation is usually calculated with very simple assumptions. Sometimes the structure of the aggregate is not even considered at all. The result of sticking particles together is then treated as being spherical and compact just like the individual monomers. While this is a reasonable assumption for the coagulation of liquid drops, it is certainly not valid in our context. More detailed calculations were done first by Wright (1987), Meakin & Donn (1988), and Bazell & Dwek (1989). Ossenkopf (1993) made a great effort to study the typical structure of aggregates formed in molecular cores without restructuring. An interesting method has been used by Weidenschilling (see, e.g., Weidenschilling, Donn, & Meakin 1988) who assumes clusters form with a fractal dimension of about 2 up to a certain size limit (in the above cited paper 0.1 cm) and then switches to more compact clusters (dimension approaching 3). While this general trend is perhaps likely, the adopted limiting sizes and fractal dimensions are arbitrary.

In particular in ballistic trajectory calculations, grains are assumed to stick where they hit. Some authors have taken into account sticking probabilities on the basis of Chokshi et al. (1993) (see, e.g., Ossenkopf 1993 or Weidenschilling & Ruzmaikina 1994). The sticking probability then leads to a simple branching in the calculation.

With a detailed and quantitative description of the contact forces, it is possible to attack the problem completely consistently. Instead of treating a cluster as a whole, every individual grain in the cluster can be treated separately.[2] Thus, we solve the equations of motion for each individual grain under the influence of the forces transmitted by all contacts of the grain with other grains. This is, of course, a computationally very expensive procedure and not likely to be used in large-scale coagulation calculations (such as formation of planets in the solar nebula) in this way. However, such an N-particle code allows us to study the processes in great detail and to derive rules and recipes that can be applied to large-scale calculations like the ones by Weidenschilling discussed above. Hence, we will use the results from the previous sections to derive a simple recipe for the formation of collisional aggregates. In this we will concentrate in deriving simple expressions describing the onset and importance of compaction and destruction in collisions between grains and aggregates.

3.1. *Numerical Model*

We have developed a numerical code that, for reasons of simplicity, is limited to two dimensions. All grains move in a plane, and rotation of grains is restricted to spin about the axis vertical to the plane of motion. This has the advantage of fast development and execution time and easy interpretation of the results. Moreover, all contacts are visible on a single picture, and it is trivial to judge where in the aggregate restructuring takes place. Except for twisting, which is similar to sliding, all relevant physical processes are included, and their importance and interaction can be evaluated.

Dust aggregates that form by collisions at such low velocities that any restructuring is avoided will have an open structure with each grain connected to other grains by only one (at the end of a "finger") or two (inside a "finger") contacts per grain. The average number of contacts in these aggregates is typically equal to the number of grains in the aggregate, independent of the fractal structure and dimension. Therefore, the distribution of energy in collisions in these aggregates occurs by transport along one-dimensional chains, and this process can be well captured by these two-dimensional calculations. What is not well modeled by these calculations is the fractal dimension actually produced by the coagulation, and we will therefore refrain from deriving this.

In the model code, we solve three equations of motion for each particle: two for motion in the plane and one for rotation. For each contact, we have to solve an additional set of equations because the contact forces cannot be simply calculated as functions of the momentary grain locations and velocities. The contact forces depend also upon the history of the grain motions. This dependence is very simple in the vertical degree of freedom: Two grains with a distance just above $R_1 + R_2$ may exchange no force at all (if they have not been in contact before) or a large attractive force (if they have been in contact and are not yet separated). In the case of tangential and torque forces, the situation is more complicated. Since both the rolling and the sliding degree of freedom show elastic behavior for small forces, the contact shows no motion over the grain surfaces for small forces. Thus, in this regime, the forces can actually be calculated from the position changes of the grains since contact was first established. We can assume that at the moment of contact formation, no stresses in the tangential and rolling degree of freedom are present and that the associated forces are zero. So, the tangential motions define stresses in the tangential degree of freedom with respect to this reference point (which can be calculated from eq. [21]) as long as there is no sliding. A similar consideration holds for rolling. However, when the forces become large enough to move the contact over the grain surfaces, the reference point (the orig-

[2] A similar approach has been described by Sablotny et al. (1995).

inal contact point) starts moving as well. We therefore have to integrate equations for the displacements in the sliding and rolling degrees of freedom for each contact. We solve in addition to the equations of motion given above two equations for δ_x and δ_{xy} that include slipping of the reference point.

The initial clusters used in the calculation are derived from a simple ballistic particle-cluster aggregation model. Before being used in the calculation, the clusters are numerically cooled in order to get rid of any vibrational energy in the contacts.

The only free parameters of the problem are the properties of the monomer grains (material and size) and the structure of initial clusters.

3.2. *Monomer-Monomer Collisions*

Initially, growth of agglomerates is dominated by monomer-monomer collisions. The values of the critical energies/velocities for sticking to occur in such a collision will determine if coagulation growth can start at all—irrespective of the constraints on monomer-aggregate and aggregate-aggregate collisional growth.

In Papers II and III, we have shown in detail that rolling and sliding are both fairly irrelevant in the collision between two single grains. In the collision of two equal nonrotating spheres, the symmetry of the process would not allow for any rolling to occur. If the spheres are different, the parameters of the collision would still have to be chosen just right: the impact parameter would have to be close to $R_1 + R_2$ in order to favor tangential motions instead of vertical rebound. Also, the collision energy needed to be close to the critical energy for sticking or breakup. In such "optimized" conditions, an icy 1000 Å sphere colliding with a fixed sphere of about the same size can roll up to one revolution around this sphere (Paper II). For smaller grains and for other materials, the possible effect becomes smaller. In some of our model calculations of collisions between an aggregate and a large grain, we find somewhat larger rolling distances owing to special geometrical effects. We will discuss this later.

Since rolling and sliding play only a minor role in the collision between two grains, the crucial question of whether the grains will stick in a collision can be studied with good accuracy by restricting the calculation to the vertical degree of freedom only. Here, the calculations from Paper I can be directly applied. When the energy in the vertical degree of freedom is smaller than the critical energy for sticking $E_{\rm stick}$, the grains will stick. If the energy is larger than this, the grains will simply bounce. The critical energy for sticking was given in equation (7). This energy can be transformed into a velocity with equation (9). In the case of two identical spheres, the critical velocity is given by the expression equation (10). However, this refers only to the vertical component of the relative velocity. Therefore, the total relative critical velocity will be somewhat larger by a factor depending upon the geometry of the collision. On average, the impact energy can be larger by a factor of 2.

3.3. *Monomer-Aggregate Collisions*

After the first small aggregates have formed by coagulation, the collision of an aggregate with a single grain will become increasingly likely. Here we actually have to study three questions: (*a*) Does the grain stick to the aggregate at a given collision velocity? (*b*) Will this collision initiate some restructuring of the aggregate? (*c*) Is the collision energy high enough to "sputter" some of the aggregated grains from the aggregate, or will the aggregate be destroyed entirely? We will illustrate these questions through some example calculations.

3.3.1. *Detailed Time Sequences of Collisions*

Figure 6 shows a time sequence of the impact of a single grain on a cluster consisting of 40 grains. The grains are all of the same size, 10^{-5} cm in radius. The material properties of ice have been used for this calculation. The impact takes place from the right with a collision velocity of 2000 cm s^{-1}. The first image shows aggregate and monomer just before the collision, and the other images show later time steps with equal time spacings between the individual frames. We can see that the grain impacts and sticks. With time, there is a small restructuring process visible: The impacting grain moves together with the first grain that it hit upward until it almost makes a second contact with another grain located there. In order to understand this in terms of the critical energies, we have to consider the reduced radius and the impact energy in the collisions. The reduced radius relevant for the contacts is $R = R_1/2 = 5 \times 10^{-6}$ cm. Since the mass of the aggregate is much larger than the mass of the impacting grain, the energy is simply given by $E_{\rm coll} = \frac{1}{2}mv_{\rm coll}^2 \approx 1.7 \times 10^{-8}$ ergs, where m is the mass of a monomer and $v_{\rm coll}$ is the collision velocity. Examining Figure 5, we find that this corresponds to the critical energy for breaking a single icy contact. This implies that the energy is slightly above the critical line for sticking (compare Fig. 4). Nevertheless, sticking occurs. The important difference is that the collision energy is quickly distributed throughout the aggregate. When the impacting grain hits the first grain in the aggregate, we may on a very short timescale view this as a collision between two single grains of the same mass. In such a collision (at least, if it is head-on as in our example), all the kinetic energy of the impacting grain is transferred to the impacted grain, and, in the frame of reference of the aggregate, the impacting grain comes to rest. In the collision of two monomers, the motion would now be carried by the impacted grain, and the contact would break again if the energy of the impact was high enough. However, since the second grain is connected to the aggregate, it transfers its energy quickly to the next grain in the chain and thus does not move away from the impaction grain. Therefore, the original contact remains. While the energy is being transferred from grain to grain, some of it is lost since each contact between grains has several degrees of freedom (see Fig. 2), each of which can be excited with a certain amount of energy. When the wave of energy reaches grains at the boundary of the aggregate, not enough energy is left to break a contact. Finally, in examining the results of this collision, we have to take into account that the aggregate is not a linear chain of grains. At oblique connections, energy transfer is not complete. Only the vertical component of the momentum is (partially) transferred to the next grain, while the grain itself continues to move with the tangential component of its motion. It is for this reason that in the example shown in Figure 6, the first contact in the aggregate that is not straight in the line of impact is the site where most rolling occurs.

We can see here already an interesting effect of coagulation onto aggregates as compared to the monomer-monomer collisions discussed above: The sticking is

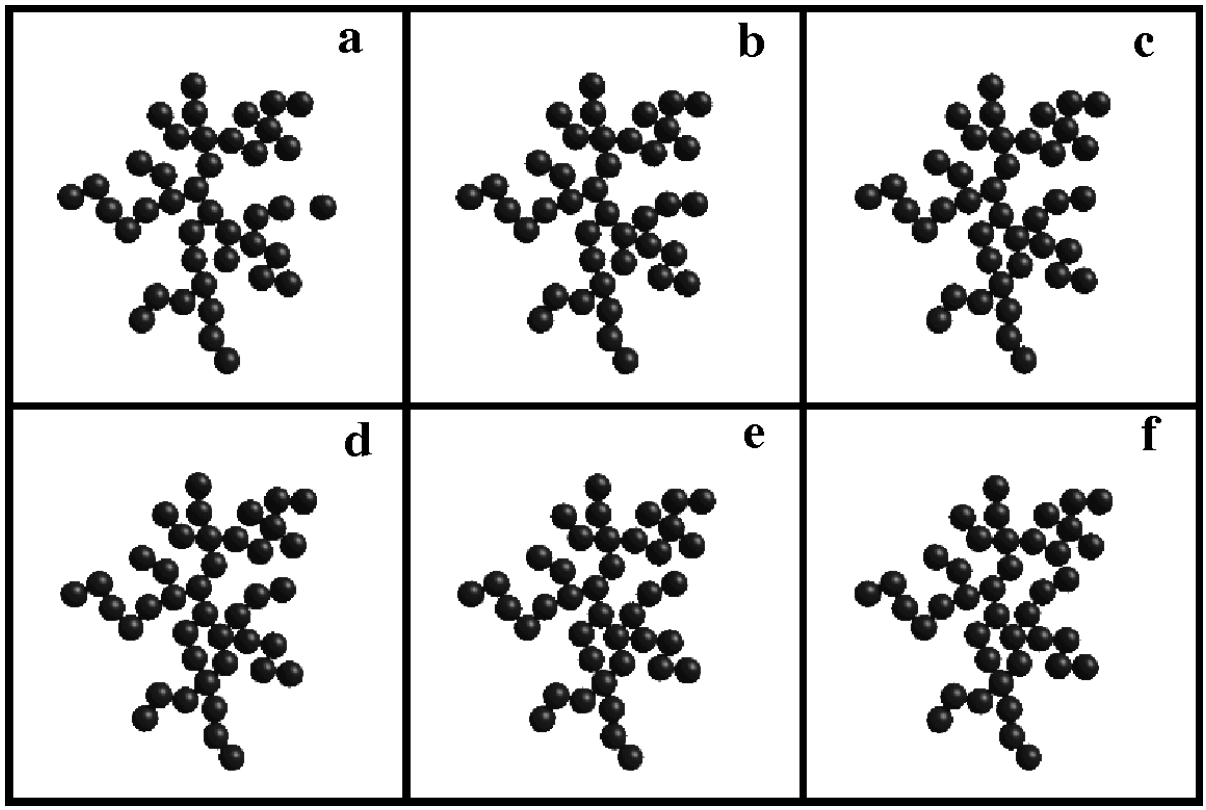

FIG. 6.—Time sequence of collision between an aggregate made of 40 grains and a single grain. The radius of individual particles is 1000 Å. The grains are made of (water) ice. The collision takes place at 2000 cm s^{-1}. The six frames cover a total time of 11.8×10^{-8} s, with 2.36×10^{-8} s steps between two frames.

enhanced when impacting on an aggregate. In general, in a coagulation process, the first step from monomers to dimers is the rate-limiting step. The conditions for sticking are met for this step; further growth will be rapid.

In Figure 7, we show another example. The collision conditions are identical to the previous case except for the collision velocity, which we have increased by a factor of 10 to 20,000 cm s^{-1}. The impact energy is now $E_{\rm coll} = 1.7 \times 10^{-6}$ ergs, a little more than 2 orders of magnitude above the energy required to break a single contact (Fig. 5). Consequently, as the energy gets distributed through the aggregate, many of the involved contacts actually break. Not all of them do, however, though the energy of the collision would in principle suffice to do that. However, a large fraction of it ends up in kinetic energy of the fragments that leave the aggregate. Another important result from this model calculation is that the impact does not lead (as one might have expected) to a large compression of the aggregate but rather immediately goes ahead and destroys it. We can see that just after the impact (Fig. 7, second frame), there are already a couple of contacts broken near the impact point, while the far end of the aggregate appears undisturbed. This means, that destruction of the contacts is immediate, basically in the first vertical vibration that the contact goes though. Because of this, there is hardly any "soft" restructuring by rolling—just destruction. We will come back to this in § 3.4.

3.3.2. *Final Results of Collisions at Different Velocities*

Figures 8, 9, and 10 summarize the results of collisions like the ones discussed above for three different material-size combinations. The first frame always shows the situation just before the impact. The impact occurs in all cases on a straight line from right to left with the velocity noted below the frame (in cgs units). The velocities of both collision partners in the up-down direction is initially zero, as is the rotational velocity about an axis perpendicular to the plot area. The other frames show the final result of a collision at a certain velocity. By final result we mean that we have followed the model calculation until the contacts have basically come to rest, i.e., until all the major rolling and breakup has stopped. Only in the highest velocity frames is rolling still going on, but we wanted to capture the fragments before they move out of the frame. In all cases, we have done model calculations for the velocities 50, 100, 200, 500, 1000, 2000, 5000, 10,000, 20,000, 50,000, and 100,000 cm s^{-1}. The velocities actually shown have been selected to represent the major changes in the collision behavior. The second frame shows (unless otherwise noted) the highest velocity with sticking but without any visible restructuring. The last frame always shows the collision velocity at which almost complete destruction of the aggregate(s) into individual grains occurs. The remaining frames 3, 4, and 5 show prominent intermediate steps.

In Figure 8 it can be seen that no visible restructuring occurs at a velocity of 500 cm s^{-1}, which corresponding to an impact energy of $E_{\rm coll} = 1.04 \times 10^{-9}$ ergs that puts it well under the energy limit for breakup in Figure 5 but inside the wedge where "visible" rolling of a single contact would be possible. Again, this does not happen, since the energy is distributed efficiently throughout the aggregate. Some restructuring near the impart point can be seen at velocities 2000 and 5000 cm s^{-1}. The 2000 cm s^{-1} collision has been inspected in detail in § 3.3.1. At 5000 cm s^{-1}, the

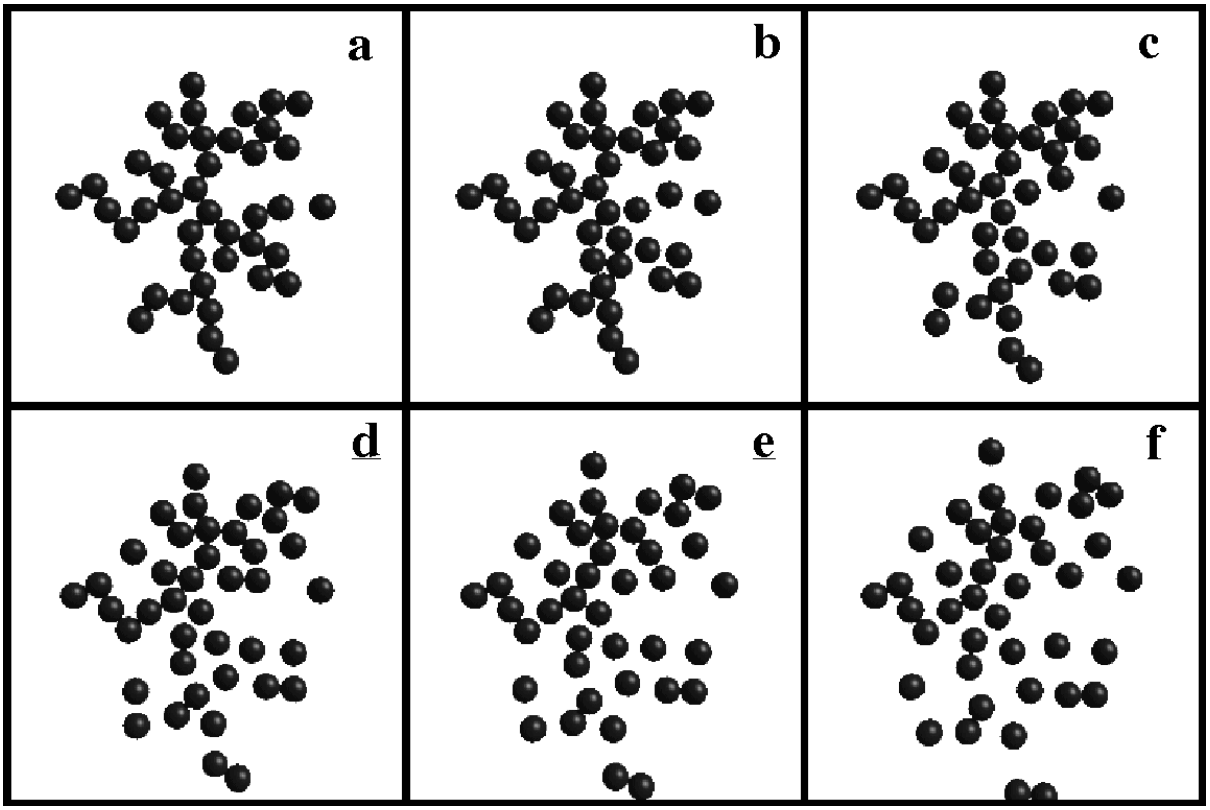

FIG. 7.—Same as Fig. 6, but for a collision velocity of 20,000 cm s^{-1}. The six frames cover a total time of 11.5×10^{-9} s, with 2.3×10^{-8} s steps between two frames.

restructuring actually already involves the breaking of a few contacts. Close inspection of the time sequence shows that the contact that connects the impacted grain with the rest of the aggregate breaks but that the two grains actually find their way upward to the next branch of the aggregate where they stick again. The energy associated with 5000 cm s^{-1} is $E_{coll} = 10^{-7}$ ergs, which puts it a factor of 10 above the critical energy for breakup (again, see Fig. 5). At 10,000 cm s^{-1}, the aggregate breaks into two large pieces and a few smaller fragments. The number of broken contacts amounts to approximately 6. At 20,000 cm s^{-1}, as discussed above, many of the contacts originally present breakup. The total number of contacts that break in this calculation is approximately 20. Therefore, the number of contacts broken appears to scale approximately with the impact energy. We will find that this also holds for other materials and other grain sizes.

3.3.3. *Effects of Grain Size and Material Properties*

It is interesting to look at the effects of grain size and grain material on the results found so far. To study this, we show similar calculations for grains with the same size but silicate material instead of ice (Fig. 9) and for ice grains with radii smaller by a factor of 10 (Fig. 10).

We had already seen in § 2 that silicate material properties lead to much smaller intergrain forces than ice properties. Furthermore, the solid wedge in Figure 4 indicating the possibility of rolling versus breakup is quite narrow for silicate material. As expected, collisions that lead to similar results will have much smaller collision velocities than in the case of ice grains (Fig. 9). The first frame shows again the situation just before the collision. The highest collision velocity without visible restructuring is at a collision velocity of only 50 cm s^{-1} as compared to 500 cm s^{-1} in the case of ice. At 100 cm s^{-1}, the first contact breaking has already occurred—the impacting grain along with the impacted grain has moved to the upper aggregate branch. At 500 cm s^{-1}, the aggregate starts to break up into large fragments, and at 1000 cm s^{-1}, it has been largely destroyed. Exactly the same exercise with critical energies can be repeated in this case—with very similar results: The highest collision energy at which no visible restructuring happens is just at the breakup energy for a single contact. The first monomer loss occurs at an impact energy about a factor of 10 larger than the breakup energy for single contacts. Again, the number of contacts broken is a linear function of the impact energy.

Figure 10 shows the results for a set of collisions with much smaller ice grains (10^{-6} cm). We had seen in § 2.3 and in Table 2 that the breakup energies scale with the 4/3 power of the reduced particle radius. Since we are dealing with a single particle size at a time, the critical velocities obviously scale (see also eq. [9]) like $R^{-5/6}$, similar to the sticking energies given in equation (10). Similar effects must therefore happen in collisions of 10^{-6} cm grains at velocities that are a factor of approximately 6 lower. This does of course neglect additional effects due to the different dependence of rolling dissipation upon the grain radii. Nevertheless, the results shown in Figure 10 fit quite well into this picture. First restructuring appears at 5000 cm s^{-1} for 10^{-6} cm ice grains, while it happens at 1000 cm s^{-1} for 10^{-5} cm grains. The aggregate breaks into pieces only at a rather high velocity of 100,000 cm s^{-1} for the small grains, while this already happens at 10,000 cm s^{-1} for the large grains.

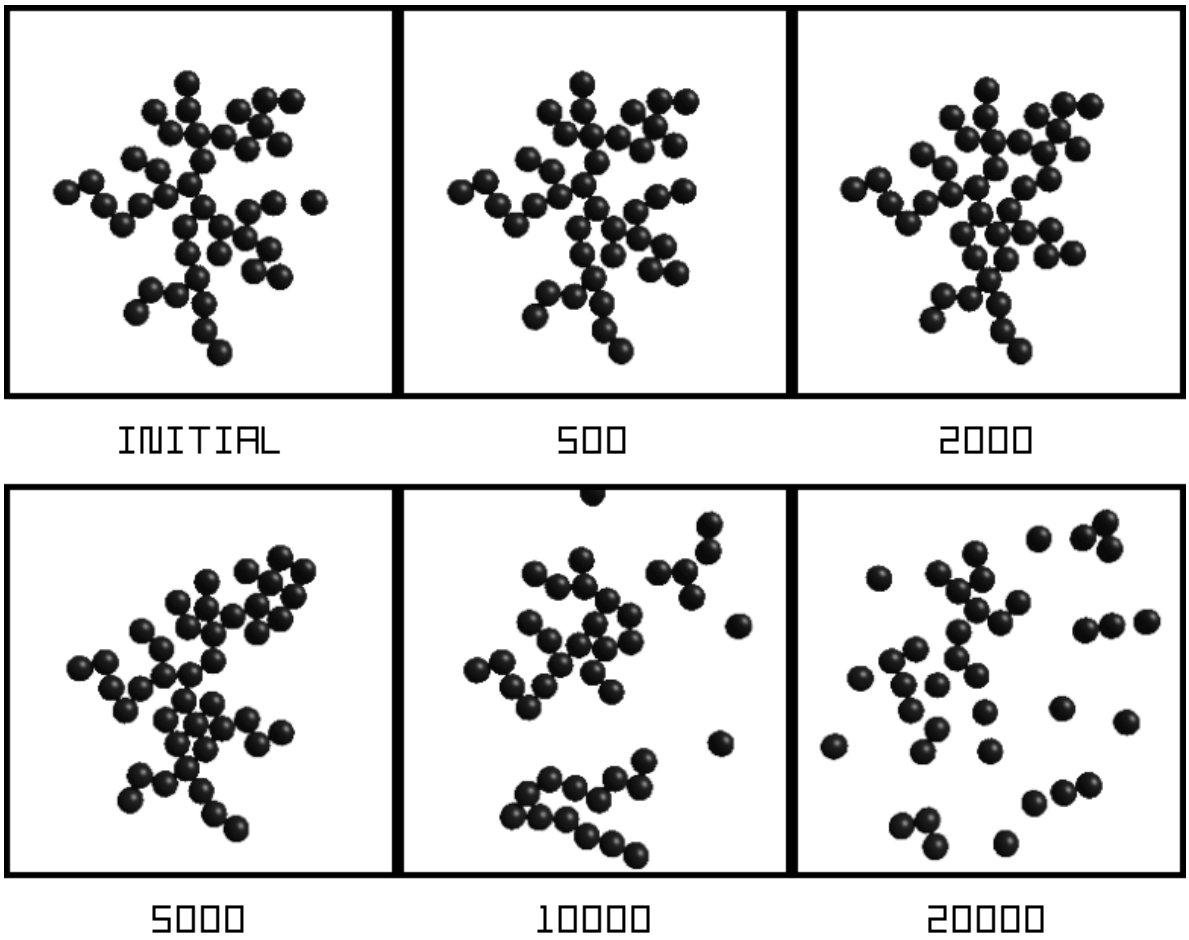

FIG. 8.—Velocity sequence for collisions of the types shown in Figs. 6–7. Thus: Impact of a single grain onto a 40-aggregate. Individual particle radius: 1000 Å. Grain material: ice. The first frame shows the situation just before the collision, and the following frames show the "final" result of the collision with the relative velocity in cm s^{-1} indicated below the frame. By "final," we mean that most of the restructuring and contact breaking has finished.

Again, if we count the number of broken contacts, it is a linear function of the impact.

3.3.4. *The Effects of a Distribution in Grain Sizes*

Up to now, all calculations have been performed for monomers of the same size. In principle, this simplification might influence the collisional outcome profoundly, particularly for those collisions that lead to complete destruction of the aggregate. When all participating particles have the same mass, the redistribution of energy is especially efficient. Therefore, after a few vibrations of the entire aggregate, the energy will be evenly distributed among the grains. This process takes longer when the grain sizes differ. Also, the contacts are not equally strong in this case, and one might expect that some contacts will be disrupted preferentially. In order to check these points, we have conducted model calculations similar to the ones above (ice grains) but with grain radii randomly distributed in the range 5×10^{-6} to 2×10^{-5} cm (Fig. 11). The impacting grain is again an icy grain with $R_2 = 10^{-5}$ cm marked by an arrow in the figure. The monomer impacts on a larger grain ($R_1 = 2 \times 10^{-5}$ cm). Thus, the impacting grain transfers its entire kinetic energy to the aggregate only if it sticks. This is the case only up to a collision velocity of 1000 cm s^{-1}. In the remaining frames, the impacting grain bounces when it hits the larger grain and takes a large part of it energy with it. In an elastic head-on collision, the energy is transferred with an efficiency

$$\varepsilon(m_1, m_2) = 4 \frac{m_1/m_2}{(1 + m_1/m_2)^2}, \tag{32}$$

where m_1/m_2 is the mass ratio of the impacted grain and the impacting grain, respectively. For a mass ratio 8/1, we find that the efficiency is approximately 0.4. Thus, 40% of the impact energy is transferred to the aggregate and is available for restructuring and destruction. At 5000 cm s^{-1}, we see some restructuring happen near the impact region. At 10,000 cm s^{-1}, the aggregate loses a member; at 20,000 cm s^{-1}, it breaks into pieces; and at 100,000 cm s^{-1}, it is largely destroyed. As expected, the weakest links in the chain break first; i.e., breakup occurs preferentially for small grains bridging two larger grains in the chain. Comparing these results with those in Figure 8, we conclude that very similar effects happen, only at somewhat higher velocities reflecting the lower energy transfer efficiency.

3.3.5. *Impact on a Large Grain that Has Small Grains Attached to Its Surface*

In Figure 12, we show the results of a small grain impacting a large grain that has many small grains attached to it. The large grain has a radius of 10^{-5} cm, while the small grains attached to its surface are 10^{-6} cm. The impacting grain is a little larger (2×10^{-6} cm). At very low velocities, the impacting grain already sticks to some of the small

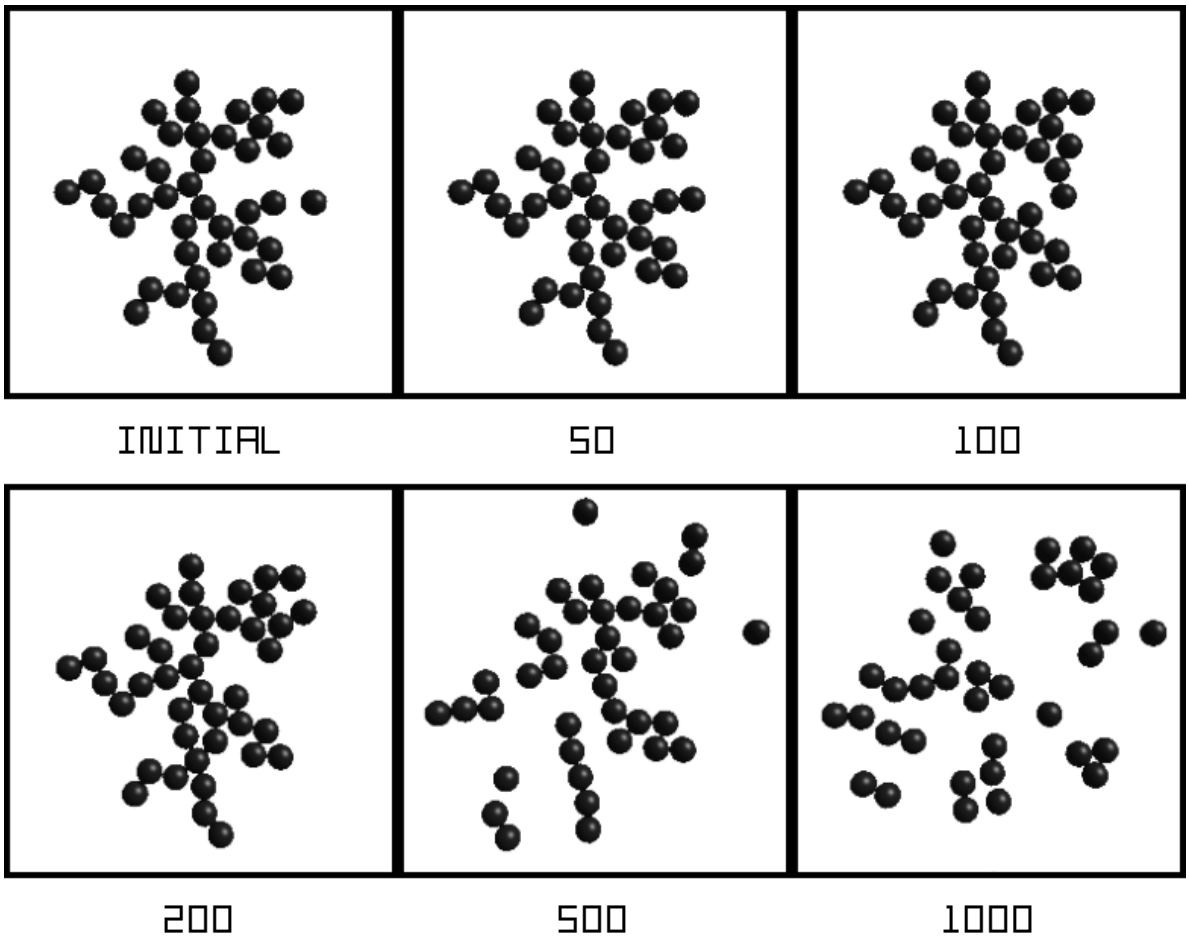

FIG. 9.—Velocity sequence. Impact of a single grain onto a 40-aggregate. Individual particle radius: 1000 Å. Grain material: silicate. Thus, it is the same as Fig. 8 but for the grain material silicate instead of ice.

grains on the surface. At 5000 cm s^{-1}, it first "penetrates" to the surface of the big grain. However, at this and at all higher velocities studied, the impact damages the aggregate only near the impact site. The small grains attached to the surface of the core grain far away from the impact region are shielded very well and are not influenced at all by the collision. This is, of course, mainly due to the high mass ratio of 125:1. Therefore, the energy transfer efficiency is only (see eq. [32]) about 3%. The highest velocity in Figure 12 would easily be sufficient to shatter the entire aggregate if all the grains were of radius 10^{-6} cm (compare Fig. 10). Thus, the one very big grain changes the results considerably. Whereas aggregates of equal sizes particles can be destroyed relatively easily, a mantle of small grains on a large grain is well protected simply by the large mass of the core grain.

3.4. *Aggregate–Large Grain Collisions*

There is one additional type of collision between an aggregate and a single grain that we have not studied so far. The impact of a large grain onto an aggregate. By large, we mean large compared to the size of the aggregate constituents. Two examples of this are shown in Figures 13 and 14, respectively. From the results of the collisions discussed so far, one might expect similar results: Sticking without restructuring at low impact energies, very little restructuring at intermediate energies, and destruction at high energies. However, this is only partially true in this case. Clearly, we can see the two extreme ends of it: Sticking without restructuring at low velocities and destruction at high velocities. If we calculate the corresponding impact energies for either pure sticking or complete destruction, they turn out to be the same as in the previously discussed collisions. But at intermediate velocities, we can now see a large amount of restructuring going on! In Figures 13 and 14, the impacting grain almost buries itself in a much compacted matrix from the constituents of the aggregate. First of all, we see that already at 200 cm s^{-1} (Fig. 13) impact velocity, there is some restructuring near the impact point, whereas in Figure 8, nothing really happens up to 500 cm s^{-1}, reflecting the much higher reduced mass in the collision. A similar consideration applies to the breakup collision (2000 vs. 10,000 cm s^{-1}).

These differences result from the differences in energy transfer during the collision. In the collisions studied in the previous sections, the entire collision energy is transferred immediately, i.e., within one collision time.[3] In a collision with a small grain, all the energy gets transferred to the first member of the aggregates that gets hit, and the energy is then transferred on a similar timescale to the next grain. The first grain hit has basically only one chance to move, which is right at the beginning. In order to move a large

[3] The collision time has been defined in Paper I as the time two grains are in contact during a bouncing collision and is typically of the order of 10^{-9} s for grains with radii of 10^{-5} cm.

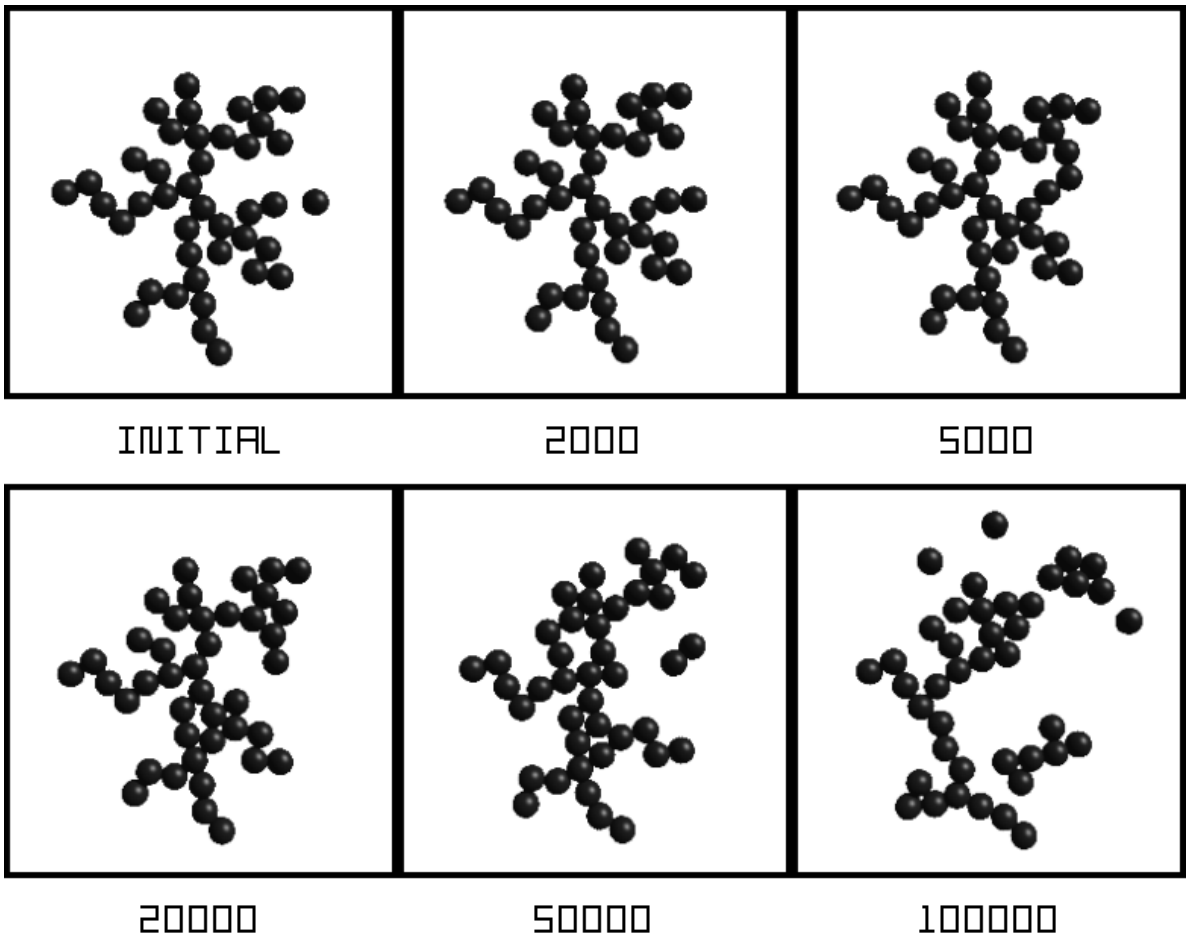

FIG. 10.—Velocity sequence. Impact of a single grain onto a 40-aggregate. Individual particle radius: 100 Å. Grain material: ice. Thus, it is the same as Fig. 8 but for much smaller grains.

amount on its own, it needs to have a kinetic energy that is comparable to the energy needed to break a contact. However, as soon as it has passed its energy on to its neighbors, it does not have enough left to move—thus, restructuring remains very limited.

In the collision with a large grain, the total collision energy is transferred over a much longer interval. Of course, the initial collision of the impacting large grain with the outermost member of the aggregate is equally short. However, only a small fraction of the energy is transmitted in this initial contact. Even if the impact velocity is high enough to let the grain bounce off the surface of the big grain, its velocity in the frame of reference of the aggregate is at most twice the impact velocity. This corresponds to an energy of $2m_1v_{\rm coll}^2$, where m_1 is the mass of the impacted aggregate member. This is only one-tenth of the collision energy (since the aggregate has 40 particles).

Subsequently, the large impacting grain moves on toward the aggregate and more or less continuously presses on one side of the aggregate. The total collision time is approximately equal to the depth the impactor penetrates into the aggregate divided by the impact velocity. The penetration depth is of the order of the size of the aggregate itself, thus some 10^{-4} cm. At an impact velocity of 1000 cm s^{-1}, this results in a collision timescale of 10^{-7} s, 2 orders of magnitude longer then the timescale mentioned above for the collision of two grains. Thus, the transfer of the kinetic energy into the internal degrees of freedom is comparatively gentle, at a rate of 1% from the collisions in Figure 8. Furthermore, the forces are more directed, since the large grain presses from the same direction all the time. This is also very different in the case of a collision with a small grain. There the directional information is lost as quickly as the energy is distributed throughout the aggregate. After the hit, all contacts are "excited" and vibrate and may even roll small distances in some direction and back but do not move consistently in a certain direction.

These two effects make a huge difference for restructuring, since rolling restructuring is already possible at energies much lower than the breakup energy for a contact (§ 2.3). So large amounts of rolling can also be achieved by supplying energy for the contact to move continuously for a long time. While this was not possible to realize in collisions with grains of the same or smaller sizes than the aggregate constituents themselves, a collision of an aggregate with a large grain provides for the correct conditions.

As discussed above, restructuring of the aggregate in a collision with a large grain starts at a lower velocity (but the same energy) than in the collision with an equal-sized grain. Likewise, destruction of the aggregate in large grain collisions also starts at the same collision energy as in the equal-sized collisions; i.e., at $\approx$2000 cm s^{-1} in Figures 13 and 14 as compared to 10,000 cm s^{-1} in Figure 8. Similarly, complete destruction of the aggregate already occurs at 5000 cm s^{-1} in the collision with the large grain, while for equal-

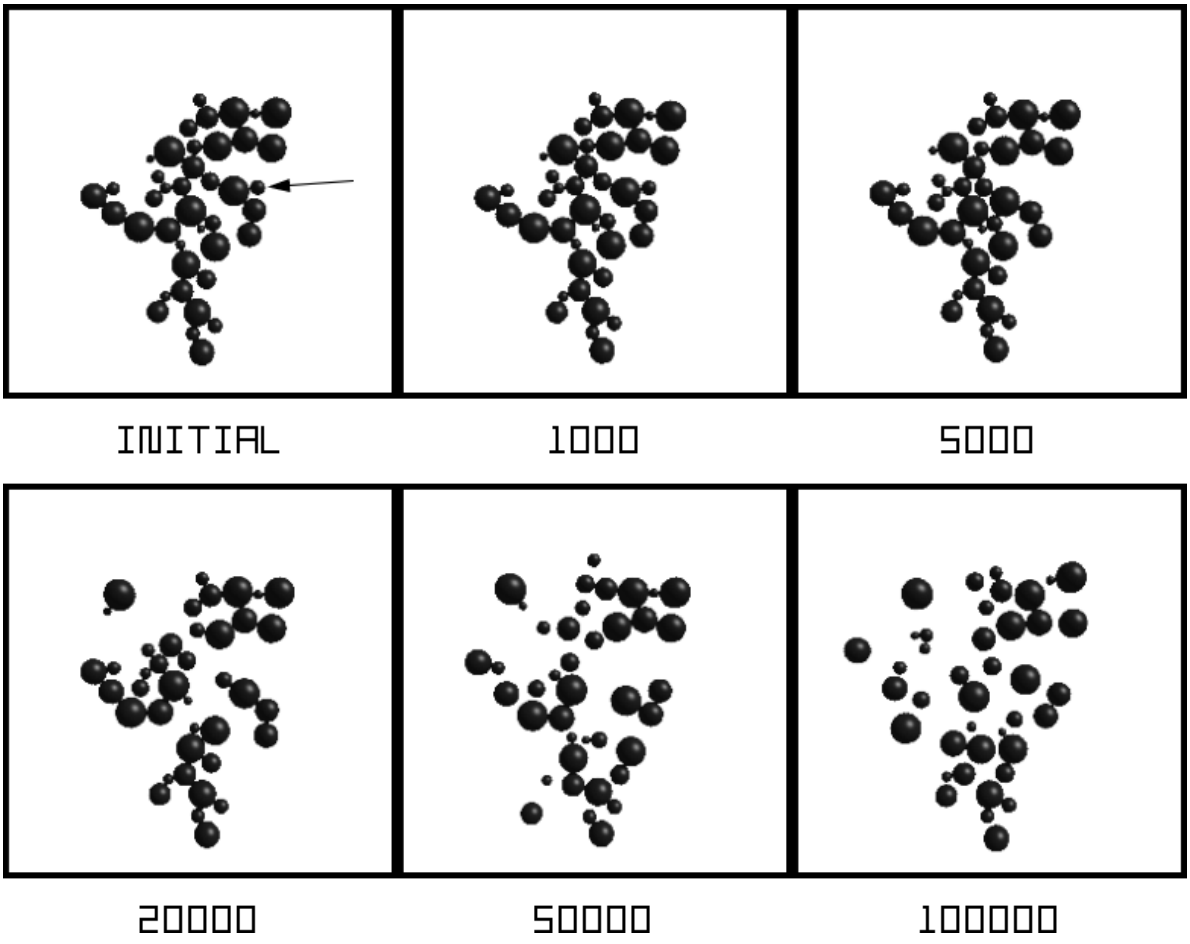

FIG. 11.—Velocity sequence. Impact of a single grain onto a 40-aggregate. Individual particle radius: in the range from 500 to 2000 Å. Grain material: ice. This figure is similar to Fig. 8, but with a range of particle sizes. The arrow in the first frame marks the impacting grain.

sized grains, this takes 20000 cm s^{-1}. Thus, in terms of energy, the limits associated with restructuring do not depend on the size of the impactor. However, the amount of compaction resulting from the collisions does. As emphasized above, the longer collision time associated with the large-grain collisions allows the rolling degree of freedom to couple better to the kinetic energy of the collision owing to the continuous pressing force. The resulting structures are therefore markedly different.

3.5. *Aggregate-Aggregate Collisions*

When considering restructuring, the collision of two aggregates is very similar to the collision of an aggregate with a big grain, and the same arguments on the efficiency of restructuring apply here as well, except that *both* aggregates are now subject to restructuring. Since the physics is very similar, only a single example of such a collision is shown (in Fig. 15). Already at 100 cm s^{-1}, some minor restructuring occurs near the impact point. The following frames show that restructuring and compression can be surprisingly efficient. At 1000 cm s^{-1}, both aggregates have been combined into a single entity in which it is difficult to decide which grain came from which aggregate. The new aggregate is much more compact than the old aggregates were. The compression is about as high as it can get by rolling, and further compression would require sliding. In these two-dimensional calculations, two contacts will stop a grain from further rolling. In three dimensions, this would be achieved only with three contacts.

3.6. *Distribution of the Impact Energy*

It is interesting to study in more detail the channels which take up the original impact energy. Obviously, the energy needs to either remain as kinetic motion of the fragments or be consumed in one of the dissipative channels. In Figure 16, the energy budget of the collisions between two equal clusters of icy grains (as seen in Fig. 15 and discussed in § 3.5) has been broken down into the different contributions. As expected, at low impact velocities without destruction, almost the entire impact energy is dissipated in the rolling degree of freedom. At the lowest velocities, there is a small part of the energy seen as kinetic motion (*solid area*). This kinetic energy reflects the vibrations in the still excited contacts that cause the particles to move relative to each other. The total amount of this vibrational energy is small, so that at somewhat higher impact energies, its fraction becomes negligible. At an impact velocity around 2000 cm s^{-1}, when the first contacts break, a fraction of up to 30% of the impact energy is used to break contacts. At the same time, we can also see that the sliding degree of freedom starts dissipating energy as well. The actual motion of the contact due to sliding remains very small, but due to the high friction forces involved, a sizable fraction of the total energy (again up to 30%) is dissipated here. That sliding starts only

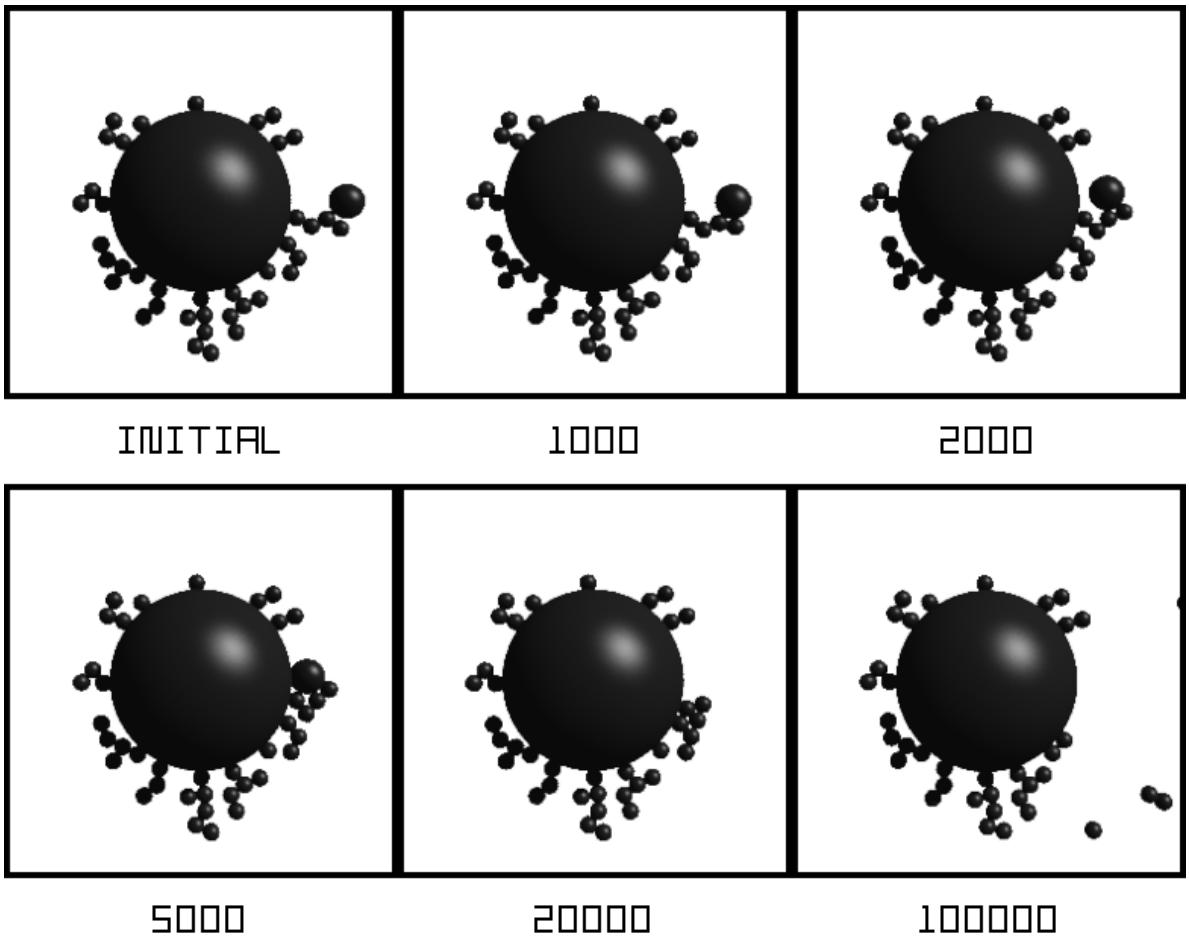

FIG. 12.—Velocity sequence. Impact of a grain (radius 200 Å) onto a larger grain (radius 1000 Å) that has small grains (100 Å) attached to its surface.

when the first contacts break is consistent with the discussion in § 2.2.2. For velocities in excess of 5000 cm s^{-1}, the aggregates break up completely. Hence, for larger velocities, the fractional energy flowing into contact-breaking energy decreases. The extra impact energy goes into kinetic energy of the fragments.

4. DISCUSSION

In the last section, we have discussed a large number of different cases for collisions between particles and/or clusters. In this section, we will attempt to pull the obtained results together into a unified scheme on cluster collisions. Our main goal is to specify the energy domains of the collisions in which specific processes occur and to formulate a set of rules for complex cluster formation by coagulation. This is quite an important task, since it seems to be out of the question for quite some time to include calculations as detailed as the ones performed here into large-scale calculations of coagulation in dense interstellar clouds or in protoplanetary disks. In these cases, one is rather interested in the structure of the produced aggregates in order to derive quantities such as porosity, fractal dimension, absorption and emission properties, aerodynamic behavior, mechanical stability, heat conduction behavior, and others.

In order to put the occurrence of critical processes in the aggregates on a common denominator, we will link them to the impact energies on one side and to the critical energies specific for the aggregates and/or their individual contacts on the other side. We will consider the following "basic" processes:

1. Sticking without restructuring.
2. First "visible" restructuring.
3. Loss of one monomer.
4. Maximum compression.
5. Catastrophic disruption.

We have performed a large number of calculations that can be subdivided into the following subcategories:

Cluster–Small Monomer Collisions.—This is the type of collision shown in Figure 8. By "small" monomer we mean that the impacting grain is at most of roughly the same size as the constituents of the aggregate. It may also be much smaller. We have performed calculations of aggregate constituent radii 10^{-5} cm and 10^{-6} cm and impactor radii of the same size and smaller down to a factor 10 smaller.

Cluster–Large Monomer Collisions.—This is the type of collision shown in Figure 14. By "large" monomer we mean that the impacting grain is larger than the constituents of the aggregate. Here we have performed calculations of aggregate constituent radii 10^{-5} cm and 10^{-6} cm and impactor radii of the same size and larger up to a size of 10^{-2} cm.

Cluster-Cluster Collisions.—This is the type of collision between two clusters of similar size (see Fig. 15). Calculations include four different materials, and aggregate constituent radii 10^{-5} cm and 10^{-6} cm.

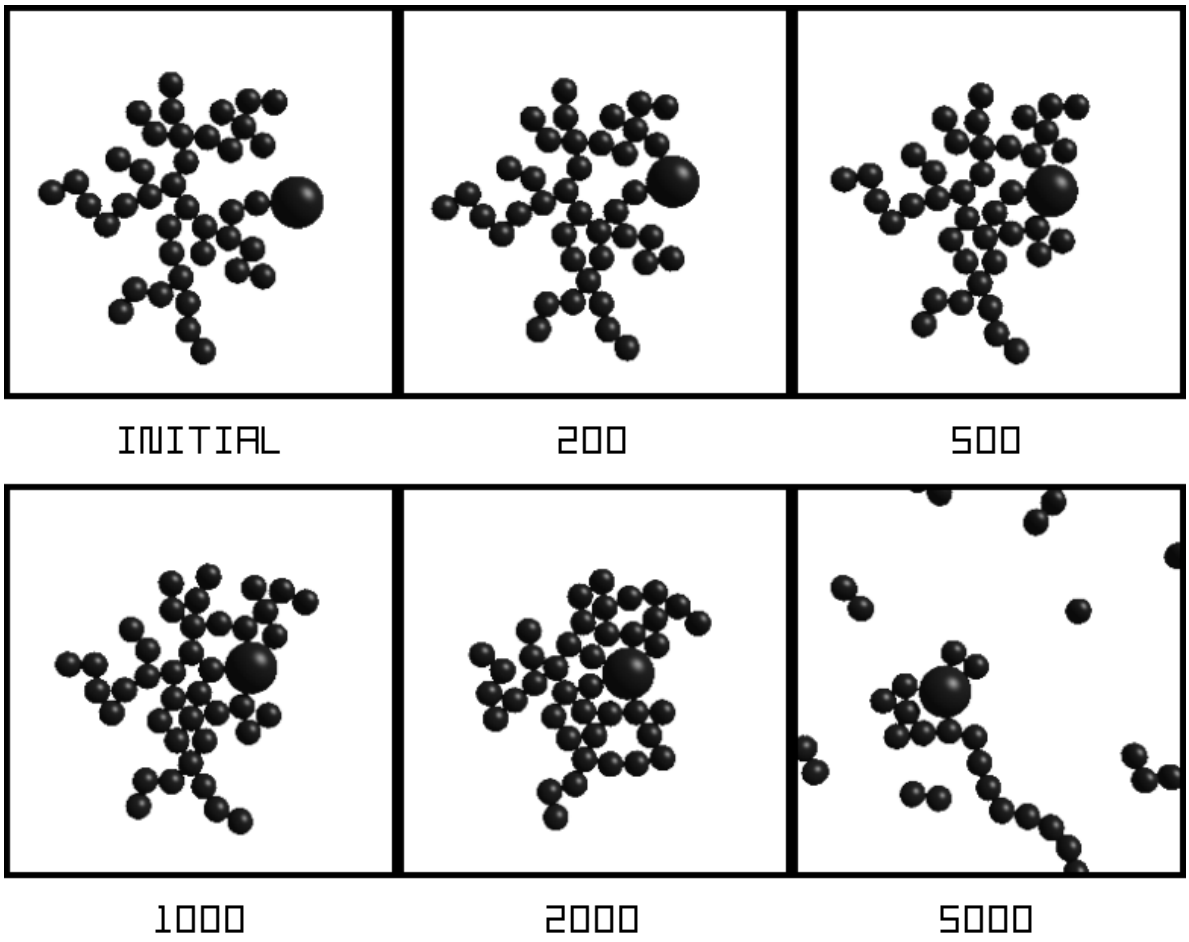

FIG. 13.—Velocity sequence. Impact of a single grain onto a 40-aggregate. Individual radius of aggregate members: 1000 Å. Radius of the impactor: 2000 Å. Grain material: ice.

Cluster with Varying Grain Sizes–Monomer Collisions.—This is the collision type shown in Figure 11. Calculations have been done for ice grains only.

Core-Mantle Cluster–Monomer Collision.—This is the collision type shown in Figure 12. A large core, surrounded by a noncompact structure of small grains, collides with another grain of arbitrary size. We have done these calculations for two different materials.

In most of these categories, we have conducted calculations for several materials in order to study the influence of material properties. For each case, a complete velocity grid from 50 to 100,000 cm s^{-1} is available.

The results of all calculations are summarized in Figure 17. At a first glance, this appears to be a rather complex figure. However, the results that can be extracted from this figure are quite simple. The figure shows the collision energy that is necessary to initiate a certain process in a collision and compares these energies with multiples of the critical energies derived in § 2.3. The horizontal axis in Figure 17 indicates the different collision categories. The suborder in each category indicates the material properties used in the model calculation. Furthermore, the plot discriminates between the two cases of a small (*open triangles*) and a large (*filled triangles*) grain hitting a cluster. Here, small grain corresponds to sizes equal to or smaller than typical aggregate member size. As we had seen in § 3.3, in these cases, restructuring usually is of minor importance. In the case of collisions with large grains (or clusters) on the other hand, restructuring *is* important.

4.1. *Sticking without Restructuring*

At very low velocities, the colliding grains/aggregates will stick together without visible restructuring. At higher velocities, restructuring will occur except if the impacting grain is smaller than the aggregate member with which it first makes contact. In the latter case, if the impact velocity of such a small grain is just above the sticking velocity, the impactor will bounce off without any visible restructuring. Therefore, we consider here only cases in which the impacting grain is not larger than the impacted grain. We have determined the highest velocity at which the grain still sticks without any destruction of contacts—whether it is the contact between the impactor and the aggregate itself or any other contact deeper in the aggregate (Fig. 17). For this process, the relevant kinetic energy involves only the two collision partners (the impactor and the impacted grain), and we neglect the mass of the rest of the aggregate for this comparison. The impact energy is then

$$E_1 = \frac{1}{2}\frac{m_1 m_2}{m_1 + m_2} v_{\rm coll}^2 , \qquad (33)$$

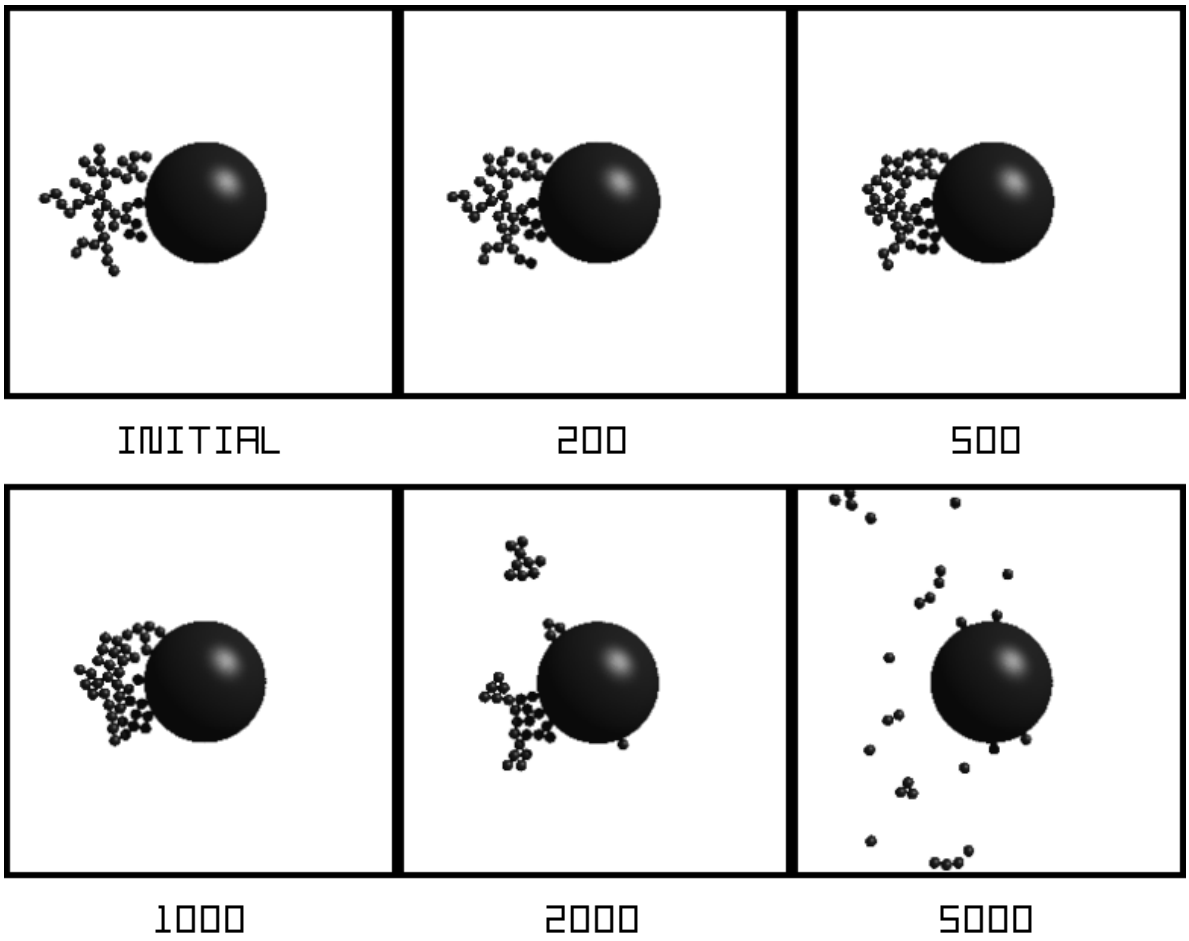

FIG. 14.—Velocity sequence. Impact of a single grain onto a 40-aggregate. Individual radius of aggregate members: 1000 Å. Radius of the impactor: 10,000 Å. Grain material: ice.

which we have ratioed with the critical energy for sticking $E_{\rm stick}$ (see eq. [7]) and plotted in Figure 17. As expected, the ratio is very close to unity in all cases. Thus, a small grain sticks to an aggregate only if the impact energy E_1 is less than or equal to the critical energy for sticking (Paper I). As we have discussed before, this consideration holds for the vertical degree of freedom only. On average, the impact energy may be higher by a factor of 2.

4.2. *Onset of Visible Restructuring*

We will define the onset of visible restructuring as the first sign of compaction of the grains near the impact point. The energy available to the restructuring process is the full kinetic energy of the two collision partners, not only the energy between the first two meeting grains. However, if the impacting grain is smaller than the first grain hit, only a fraction ε of the impact energy will actually be transmitted in the collision (see eq. [32]), which will result in an effective collision energy $E_{\rm eff}$ (defined later in eq. [35]).

The onset of restructuring is determined by the critical energy required to do visible rolling for a single contact (see eq. [15]). Thus, we have ratioed the $E_{\rm eff}$ with $E_{\rm roll}$ (Fig. 17). Because some of the collision energy is transported away from the impact point into the inner parts of the aggregate and stored as vibrational energy, the collision energy should slightly exceed the minimum energy for restructuring. Our model calculations show that approximately 2–10 times $E_{\rm roll}$ is necessary to produce visible effects, largely independent of collision category or material properties.

4.3. *Loss of One Monomer*

Another step on the energy scale of a collision that can be easily distinguished is the loss of one monomer. The relevant energy scale is now the critical energy for breaking one contact, $E_{\rm break}$, times the total number of contacts, n_c, in the aggregate. The total number of contacts enters here because the collision energy is quickly distributed over all contacts. The results of our model calculations are summarized in the third row of Figure 17. While the influence of the material properties is well represented by $E_{\rm break}$, the results seem to vary considerably with the collision category. In collisions of a single small grain (*open triangles*), the collision energy required to separate a monomer from the cluster is $\approx 0.3 \times n_c E_{\rm break}$, thus somewhat smaller than $n_c E_{\rm break}$. This is simply due to statistics: even though on average each contact gets less than the critical energy, the statistical fluctuations eventually concentrate more than the breakup energy in a contact. The situation is different if a cluster is hit by something big (another cluster or a big grain—Fig. 17 [*filled triangles*]). In this case, the collision energy needed to split off a monomer is about $1 \cdots 3 \times n_c E_{\rm break}$, somewhat larger than $n_c E_{\rm break}$. This may be readily understood if we

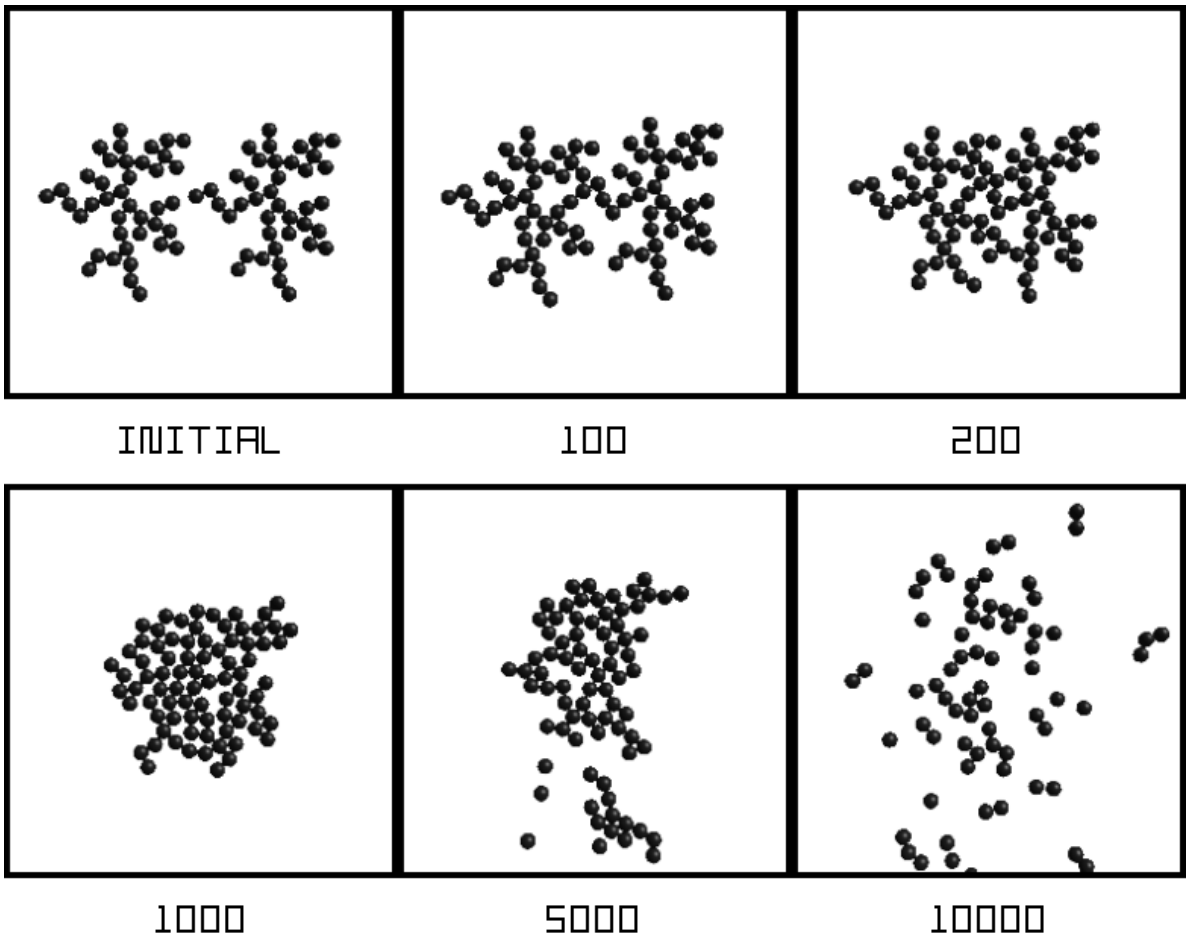

FIG. 15.—Velocity sequence. Impact of two equal 40-aggregates at different velocities. The first frame shows the situation just before the impact. The other frames show the "final" result of collisions with the velocity indicated below the frame. Grain material is ice; individual particle radius is 1000 Å.

remember that this type of collision also produces considerable compaction prior to releasing a monomer (see, e.g. Fig. 15). Therefore, a fraction of the collision energy is dissipated by restructuring processes. Since the energy required for (large distance) rolling is of the same order as the breakup energy (Fig. 4), the energy needed to separate a monomer is consequently larger.

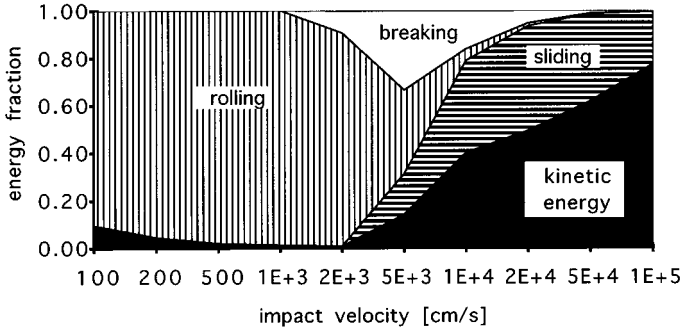

FIG. 16.—Distribution of the available energy in the collisions of two icy clusters (see Fig. 15). The plot shows the fraction of the total available energy (collision energy + binding energy of newly formed contacts) that is left behind as kinetic energy of the fragments or dissipated by rolling, sliding, and breaking of contacts, respectively. The kinetic energy includes both linear motion and rotation.

Collisions involving core-mantle clusters do not adhere to this description; the energy required for monomer loss varies over several orders of magnitude depending on the impactor size. In this case, the large grain at the center of the core mantle grain absorbs most of the impact energy, and monomers are lost only through direct hits or at very high energies at which the acceleration of the large grain is so large that contacts are broken.

4.4. *Maximum Compression*

Relevant compression occurs only in collisions between a cluster with another cluster or a big grain. Our calculation shows that maximum compression occurs when the collision energy is equal to $n_c E_{\rm roll}$ (Fig. 17). This is completely in line with our discussion on the onset of compression (see § 4.2).

4.5. *Catastrophic Disruption*

We call the outcome of a collision a *catastrophic disruption* if the colliding aggregate(s) are dissolved into monomers and very small fragments. To be precise, we require that a catastrophic disruption breaks at least half of the contacts in the aggregate(s). Thus it is not simply a breakup of the clusters into several large pieces. The results show that the energy needed to produce catastrophic disruption

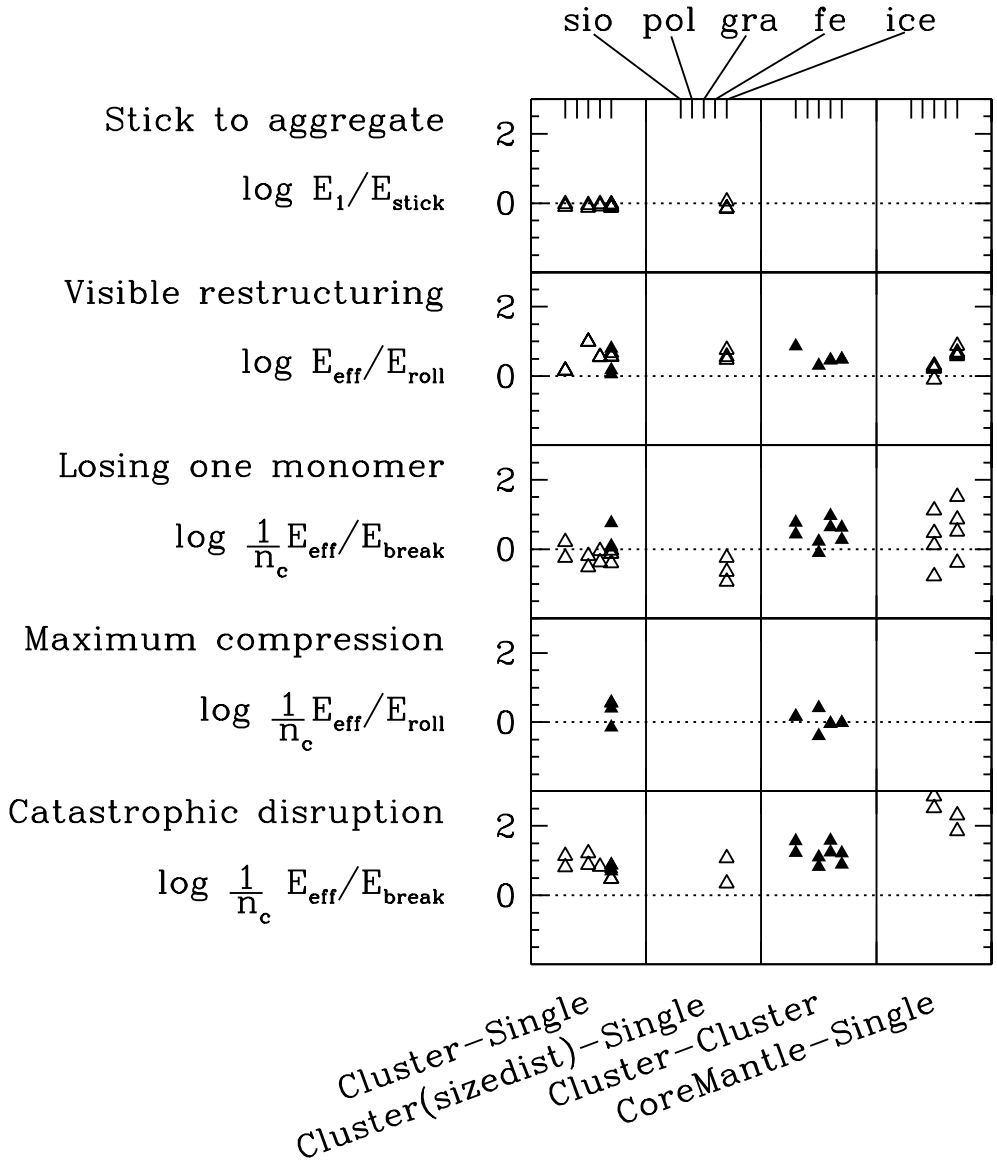

FIG. 17.—Collected results from over 300 grain/aggregate collision models. From left to right, the results are ordered by the collision category. Within each category, the horizontal offset of a point indicates a material (see labels on top of the figure). The rows of the figure indicate different characteristic processes, such as sticking of a single grain to an aggregate, start of restructuring, etc. See text for more details. The plot shows the effective impact energy (see text for definition) in relation to the critical energy for the respective process. The nice horizontal line-up of the data points indicates that the different processes are well described by the introduction of critical energies for each process.

is typically a factor of 10 higher than the minimum energy to break all bonds ($n_c E_{break}$). The remaining energy goes into kinetic motion of the dispatched monomers. Again, the factor of about 10 does not depend on the collision category or the material properties. The only exception is given by the core-mantle grains for much the same reasons as discussed in § 4.3.

4.6. *Cluster Size Scaling of the Critical Processes*

There is one remaining question: How does the critical energy required to initiate one of the processes above scale with the number of contacts in the clusters? Unfortunately, we cannot give a clear answer to that question from our model calculations since the range in cluster sizes covered so far is too small (for computational reasons). Clearly, the critical energy for sticking does not depend upon cluster size. Also, visible restructuring is a process local to the impact region and will not depend largely upon the size of the cluster. Maximum compression needs a certain amount of energy per contact in order to provide for an average rolling distance of πR. Thus, the energy to achieve maximum compression is proportional to the number of contacts as well.

However, the situation is more difficult for the loss of one monomer or for the catastrophic disruption process. As we have seen, in both cases the impact energy is distributed throughout the aggregate. Thus, the loss of a single monomer or the disruption are not the immediate and local consequence of the impact. Instead, the whole cluster is "heated" until statistical redistribution concentrates enough energy in some contacts to break them. This should probably be viewed as an evaporation process. Numeri-

cally, we find that the energy needed to trigger both the loss of a single monomer and the catastrophic disruption scale approximately linearly with the number of contacts. However, it should be kept in mind that this is only an approximate result that (presumably) cannot be scaled to arbitrary aggregate sizes. For the time being, we do not recommend extrapolating these results to aggregate sizes of more than 10^4 grains.

Another limitation for scaling of the results is of course that the impact velocities must remain in a range ion which the particle can still be viewed as elastic spheres. In particular, when the impact velocity exceeds the sound speed in the grain materials (typically a few km s^{-1}), the impact will create a shock wave in the grains leading to shattering or evaporation (Tielens et al. 1994). Impacts of such high speeds are not covered by our current model. Studies of high-speed impacts onto aggregates are now under way.

4.7. *A Recipe for Calculating Grain Coagulation*

The consistent scaling of the different restructuring effects with associated critical energies can be summarized in the following "recipe" for creating dust aggregates with restructuring effects included. These rules are intended for use in model calculations of dust coagulation in which it would be too expensive to perform detailed calculations like those carried out for the current paper. Necessarily, as a recipe, it captures only the essence of the processes involved, not the details.

Two cases can be distinguished:

1. A small grain is hitting a cluster. Small means that the grain is smaller than or at most of equal size as the typical grain in the cluster.
2. A big grain or another cluster is hitting a cluster. Big means that the impacting grain is larger than the typical grain in the cluster.

Without loss of generality, we assume that the impactor is always the less massive of the two colliding aggregates/grains. Let M_1 be the mass of the bigger cluster and M_2 be the mass of the impacting grain or cluster. Let m_1 be the mass of the first grain in cluster 1 that makes contact. The energy of the initial collision between that grain and the impactor is given by

$$E_1 = \frac{1}{2}\frac{m_1 M_2}{m_1 + M_2} v_{\rm coll}^2 , \tag{34}$$

and the effective collision energy is

$$E_{\rm ff} = \begin{cases} \dfrac{1}{2}\dfrac{M_1 M_2}{M_1 + M_2} v_{\rm coll}^2 & M_2 \geq m_1 \\ \dfrac{1}{2}\,\varepsilon\,\dfrac{m_1}{m_2}\dfrac{M_1 M_2}{M_1 + M_2} v_{\rm coll}^2, & M_2 < m_1 \end{cases} \tag{35}$$

where $v_{\rm coll}$ is the collision velocity, and the energy transfer efficiency ε(mass ratio) is defined in equation (32). This effective collision energy should be compared to energies $E_{\rm stick}$ (eq. ([7]) for the first contact between the two collision partners) and $E_{\rm break}$ and $E_{\rm roll}$ (eqs. [8] and [15]) for the typical contact in the colliding aggregate[s]). The final parameter going into this consideration is the number of contacts, n_c involved (total, in both aggregates).

Depending on where the effective collision energy lies relative to the critical energies, different outcomes will be the result, as summarized in Table 3. Relevant limiting energies are plotted for two astrophysically relevant materials in Figure 18. These calculations have been performed for a total of 100 involved contacts (thus, approximately 100 individual grains if the aggregates are still uncompressed). The critical energies are plotted as a function of the reduced radius (characteristic for the contacts, i.e., *individual* grains, in the aggregates, not for the aggregates as a whole!). The three dashed lines scale approximately linearly with the number of involved contacts, while the solid lines are independent of n_c (see, however, our comments in § 4.6). Note that the energies are not always ordered the same. In particular, in the case of small ($<10^{-5}$ cm) silicate grains, the energy to achieve maximum compression is greater than the energy required to lose at least one monomer in a collision; thus, maximum compression can never be possible in this case without losing grains.

4.8. *The Structure of Aggregates in Space*

From the critical energy criteria, we can already draw some conclusions on the structure of aggregates in astrophysically important situations. The energies required to do restructuring are clearly not available during the first stages of growth of dust particles in the protoplanetary disk. The relative velocities of all grains in the solar nebula have been calculated by Weidenschilling & Cuzzi (1993). Typical collision velocities for subcentimeter grains are only in the cm s^{-1} range and will lead to a compression-free buildup of aggregates.

Compression will, however, become important as the particles get bigger. In fact, the restructuring mechanisms discussed in this paper show that a noncompact aggregate can store and dissipate a large amount of kinetic impact energy in its internal degrees of freedom (the contacts). The capacity of this dissipation mechanism is of the order of the breakup energy $E_{\rm break}$ times the number of contacts in the aggregate, which is roughly proportional to its mass. This offers a solution to the long-standing problem of sticking of large (meter-sized) bodies in the theory of planetesimal formation (for a discussion, see, e.g., Weidenschilling & Cuzzi 1993). If these bodies were solid spheres that could be treated with the formalism of Paper I, a simple analysis shows that sticking of 1 m objects would be possible only at velocities of less than 10^{-3} cm. It is beyond doubt that this is not realistic in the solar nebula. However, as aggregates, the bodies would not act like elastic solids but rather like compressible solids with the capacity to dissipate large amounts of energy internally. Collisions between such bodies will be quite inelastic and therefore might well lead to sticking. Just as the number of contacts, the amount of energy that could be dissipated increases linearly with the mass of (number of contacts in) the bodies. Therefore, we expect that the critical velocities for sticking, restructuring, and disruption remain largely the same, i.e., of the order of a few 1000 cm s^{-1}. This would permit sticking at the velocities expected for meter-sized object in the solar nebula. A more quantitative treatment of this process will be the subject of a forthcoming paper.

Although not relevant for small aggregates in the solar nebula, restructuring may well be important in the interstellar medium, where turbulent velocity fields and low gas densities permit much higher relative velocities between dust grains, in particular dust grains of different sizes. To illustrate this, we have performed a model calculation in

TABLE 3

RULES FOR CLUSTER COLLISIONS WITH RESTRUCTURING

ENERGY	OUTCOME OF COLLISION	
	Small Grain → Cluster	Big Grain/Cluster → Cluster
$E_1 < E_{\rm stick}$	Impacting small grain sticks to cluster	
$E_1 > E_{\rm stick}$	Impacting small grain bounces off	
$E_{\rm eff} < 5E_{\rm roll}$	Sticking or bouncing off without visible restructuring of aggregate	Sticking without visible restructuring
$E_{\rm eff} > 5E_{\rm roll}$	Onset of visible restructuring local to the impact area	
$E_{\rm eff} > 0.3n_c E_{\rm break}$	Start losing monomers	
$E_{\rm eff} > 3n_c E_{\rm break}$		Start losing monomers
$E_{\rm eff} \approx 1n_c E_{\rm roll}$		Maximum compression
$E_{\rm eff} > 10n_c E_{\rm break}$	Catastrophic disruption	

which we consider the formation of an aggregate in an interstellar cloud. The aggregate is constructed from icy grains with an MRN size distribution (Mathis, Rumpl, & Nordsieck 1977). We have carried out two calculations with exactly the same sequence of grains impacting onto the aggregate.

In the first case, the velocities were all assumed to be very small. The resulting aggregate is shown on the left-hand side of Figure 19 and has the typical "fingery" structure of a ballistic particle-cluster aggregation product. The (two-dimensional) porosity of this aggregate is given by approximately 66%.

In the second case, the impact velocities were calculated under the assumption of a turbulent velocity field with maximum gas velocity $v_{\rm max} = 5 \times 10^4$ cm s^{-1} on a length scale $l_{\rm max} = 10^{18}$ cm. The gas density was 10^4 cm^{-3}, and the gas temperature was 20 K. We have used the approximate formula given by Draine (1985) to calculate the impact velocities. The results of this experiment are shown on the right-hand side of Figure 19. Clearly, the resulting aggre-

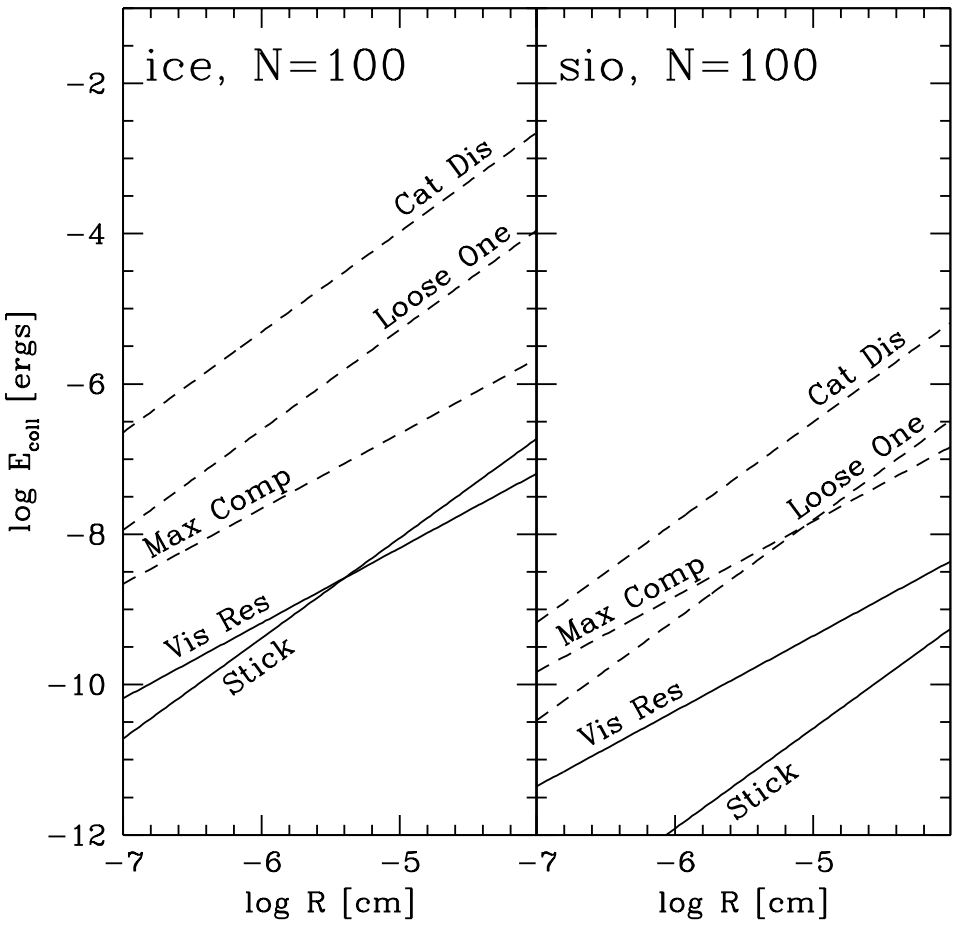

FIG. 18.—Critical energies for a collision involving 100 icy or silicate grains as a function of reduced radius typical for the individual contacts in the aggregate(s). The meaning of the different lines is discussed in the text. The dashed lines scale in energy with the number of involved contacts (≈number of grains) while the solid lines are independent of this (see, however, § 4.6). Note that the curve labeled Stick applies only to a collision of a *small* grain (for definition, see text) with an aggregate. The curve labeled Max Comp applies only to a collision of an aggregate with a *big* grain or aggregate (for definition see, text).

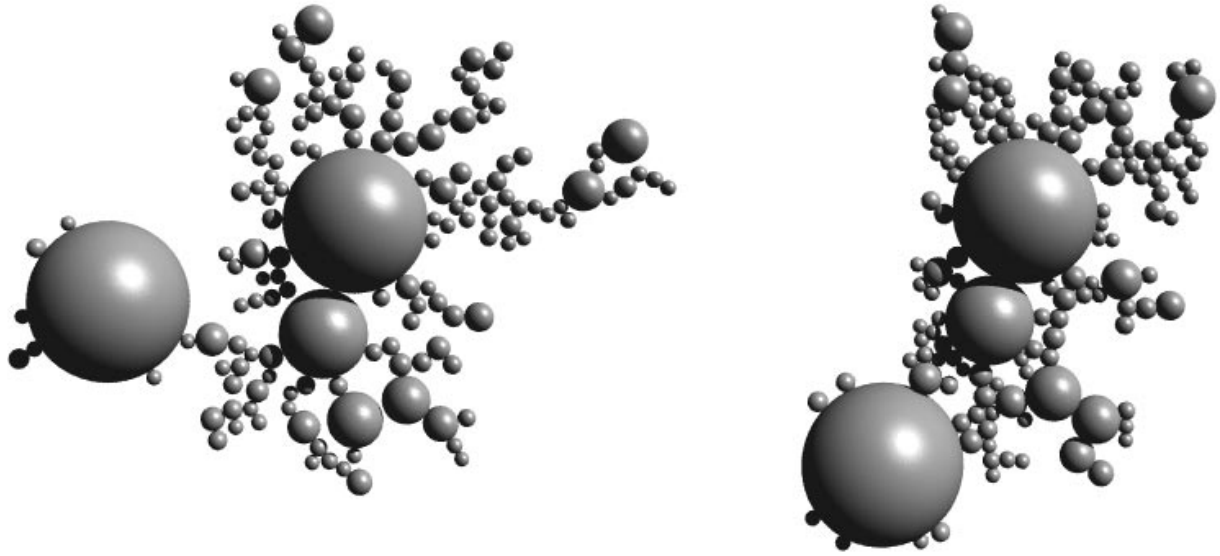

FIG. 19.—Comparison between two dust aggregates (grain material: ice) formed by an identical sequence of impacts of single grains randomly chosen from an MRN size distribution. The cluster on the left represents the result of very low velocity impacts and has not suffered any restructuring. The cluster on the right was formed in a turbulent velocity field and shows strong compression.

gate is considerably compacted, in some parts of the aggregate to the limits possible with pure rolling restructuring. The overall porosity of this aggregate is now only 53%—a large step for a two-dimensional aggregate. The compaction occurred mainly during the impact of the larger grains but also when intermediate-sized grains hit a site with many small grains.

The compaction achieved in this calculation is probably close to the maximum that can be obtained in a PCA aggregation with an MRN size distribution, since in our calculation the impact energies were not much lower than the disruption energies. In reality, the structure of aggregates in space will be in between the two cases shown here, depending upon the conditions under which they were formed. This clearly shows that neither assumption of very fractal grains as resulting from CCA nor very compact grains in which the aggregated grains are compressed to near bulk density will give a realistic description of interstellar aggregates.

5. CONCLUSIONS

In this paper we have shown and discussed the results from a detailed study of grain agglomeration. The basis for this study is a description of the physics of grain-grain contacts. Every contact between two individual grains has 6 degrees of freedom: one pull-off, two rolling, two sliding, and one twisting. Our model includes forces, stresses, and energy dissipation in all of these degrees of freedom and therefore allows for the first time a theoretical assessment of restructuring processes in aggregates on the basis of contact physics. It was shown that restructuring of dust aggregates needs to rely on rolling. The forces required to initiate sliding are generally of the same order as or higher than the forces required to break a contact. Thus, aggregates can only be restructured without being destroyed by rolling.

The contact physics was used to assemble a numerical model of dust aggregates in which the aggregates are not treated as a whole but as an assembly of N grains that are all free to move under the restrictions imposed by neighboring grains and subjected to the forces transmitted through the contacts. We have studied many different collisions of a small dust aggregate with monomers, large grains, and other aggregates. The results showed the following:

1. Sticking of impacting single grains to an aggregate is improved relative to monomer-monomer collisions, since some of the impact energy can be transferred into internal degrees of freedom of the aggregate.
2. The impact of a small single grain onto an aggregate produces only little restructuring (very local to the impact point) as long as the impacting grain is of the same size as or smaller than the average grain in the aggregate.
3. In high-velocity impacts of such small grains, the aggregate breaks into several fragments or is destroyed entirely, depending on the impact energy.
4. When an aggregate collides with a grain much larger than the average grains in the aggregate, restructuring can be efficient, and a compact aggregate can be produced in the collision.
5. When two similar aggregates collide, compaction can also be efficient.

We have summarized these results in a recipe for calculations of grain coagulation. As a function of impact energy, this recipe predicts the outcome of collisions between aggregates (and monomers).

Note.—Since the processes happening during collisions can be judged much better from moving pictures than from still snapshots, we have made available a few MPEG-I stream files at http://www.strw.LeidenUniv.nl/~dominik/Coagulation.

We would like to thank J. Cuzzi and E. Asphaug for frequent and encouraging discussions. B. Hogan provided help with computer animation of the numerical results. The figures of aggregates were created with the RAYSHADE ray tracer, written by Craig Kolb. We thank Stu Weidenschilling for a careful review of the manuscript. One of the authors (C. D.) was supported during this work by the National Research Council. Theoretical studies of interstellar dust at NASA Ames is supported under task 399-20-01-30 through NASA's Theory Program.

REFERENCES

Anderson, H. L., ed. 1981, Physics Vademecum (New York: AIP)
Austin, L. G., Klimpel, R. R., & Lockie, P. T. 1984, Process Engineering of Size Reduction in Ball Milling (New York: American Institute of Mining, Metallurgical, and Petroleum Engineers)
Bazell, D., & Dwek, E. 1989, ApJ, 360, 142
Beke, B. 1981, The Process of Fine Grinding (The Hague: Nyhoff)
Brocklehurst, J. E. 1977, Phys. Chem. Carbon, 13, 145
Brownlee, D. E. 1979, Rev. Geophys. Space Phys., 17, 1735
Chokshi, A., Tielens, A. G. G. M., & Hollenbach, D. 1993, ApJ, 407, 806 (Paper I)
Dominik, C., & Tielens, A. G. G. M. 1995, Phil. Mag. A, 72, 783 (Paper II)
———. 1996, Phil. Mag. A, 73, 1279 (Paper III)
Draine, B. T. 1985, in Protostars and Planets II, ed. D. C. Black & M. S. Matthews (Tucson: Univ. of Arizona Press), 621
Easterling, K. E., & Thölen, A. R. 1972, Acta Met., 20, 1001
Hertz, H. 1896, Miscellaneous Papers (New York: Macmillan)
Hucknal, D. J. 1985, Chemistry of Hydrocarbon Combustion (New York: Chapman and Hall)
Israelachvili, J. 1992, Intermolecular and Surface Forces (London: Academic)
Johnson, K. L. 1989, Contact Mechanics (Cambridge: Cambridge Univ. Press)
Johnson, K. L., Kendall, K., & Roberts, A. D. 1971, Proc. R. Soc. London, 324, 301
Jones, A. P., Tielens, A. G. G. M., & Hollenbach, D. J. 1996, ApJ, 469, 740
Kendall, K. 1980, Contemp. Phys., 21, 277
———. 1993, in Powders and Grains, ed. C. Thornton (Rotterdam: A. A. Balkema), 25
Kendall, K., Alford, N. M., & Birchall, J. D. 1987, Nature, 325, 794
Kendall, K., & Padget, J. C. 1987, J. Adhesion, 22, 39
Kittel, C. 1976, Introduction to Solid State Physics (New York: Wiley)
Kozasa, T., Blum, J., & Mukai, T. 1992, A&A, 263, 423
Landmann, U., & Luedtke, W. D. 1993, in Scanning Tunneling Microscopy III, ed. R. Wiesendanger & H.-J. Güntherodt (New York: Springer), chap. 9, p. 207
Markiewicz, W. J., Mizuno, H., & Völk, H. J. 1991, A&A, 242, 286
Marlow, W. H. 1980, Aerosol Microphysics I (Berlin: Springer)
Mathis, J. S., Rumpl, W., & Nordsieck, K. H. 1977, ApJ, 217, 425
Mathis, J. S., & Whiffen, G. 1989, ApJ, 341, 808
McClelland, G. M. 1989, in Adhesion and Friction, ed. M. Grunze & H. J. Kreuzer (Berlin: Springer), 1
Meakin, P. & Donn, B. 1988, ApJ, 329, L39
Nedderman, R. M. 1992, Statics and Kinematics of Granular Materials (Cambridge: Cambridge Univ. Press)
Ossenkopf, V. 1993, A&A, 280, 617
Rhodes, M. J. 1984, Principles of Powder Technology (New York: Wiley and Sons)
Richardson, D. C. 1995, Icarus, 115, 320
Sablotny, R. M., Kempf, S., Blum, J., & Henning, T. 1995, Adv. Space Res., 15, 55
Singer, I. L., & Pollock, H. M., ed. 1992, Fundamentals of Friction: Macroscopic and Microscopic Processes (Dordrecht: Kluwer)
Smyth, K. C., & Miller, J. H. 1987, Science, 236, 1540
Sperling, G. 1964, Ph.D. thesis, Technische Hochschule Karlsruhe, Karlsruhe
Tielens, A. G. G. M. 1989, in IAU Symp. 135, Interstellar Dust, ed. L. Allamandola & A. G. G. M. Tielens (Dordrecht: Kluwer), 239
Tielens, A. G. G. M., McKee, C. F., Seab, C. G., & Hollenbach, D. J. 1994, ApJ, 431, 321
Tománek, D. 1993, in Scanning Tunneling Microscopy III, ed. R. Wiesendanger & H. J. Güntherodt (New York: Springer), chap. 11, page 269
Veale, C. R. 1972, Fine Powders (New York: Wiley and Sons)
Weidenschilling, S. J., & Cuzzi, J. N. 1993, in Protostars and Planets III, ed. E. H. Levy & J. I. Lunine (Tucson: University of Arizona Press), 1031
Weidenschilling, S. J., Donn, B., & Meakin, P. 1988, in The Formation and Evolution of Planetary Systems, ed. H. A. Weaver & L. Danly (Cambridge: Cambridge Univ. Press), 131
Wiesendanger, R., & Güntherodt, H.-J., ed. 1993, Scanning Tunneling Microscopy III (New York: Springer)
Weidenschilling, S. J., & Ruzmaikina, T. V. 1994, ApJ, 430, 713
Wright, E. L. 1987, ApJ, 320, 818
Zisman, W. A. 1963, Ind. Eng. Chem., 55, 19